Journal of Computational and Applied Mathematics 234 (2010) 418–436

Contents lists available at ScienceDirect

Journal of Computational and Applied Mathematics

journal homepage: www.elsevier.com/locate/cam

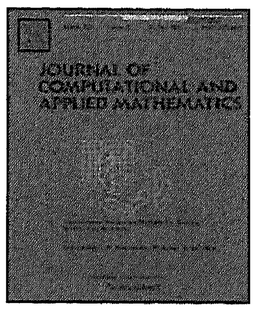

Computation of symbolic dynamics for one-dimensional maps

Lorenzo Sella *, Pieter Collins

Centrum voor Wiskunde en Informatica, Postbus 94079, 1090 GB Amsterdam, The Netherlands

ARTICLE INFO

Article history:
Received 23 June 2009
Received in revised form 13 November 2009

Keywords:
One-dimensional map
Kneading theory
Symbolic dynamics
Interval arithmetic

ABSTRACT

In this paper we design and implement rigorous algorithms for computing symbolic dynamics for piecewise-monotone-continuous maps of the interval. The algorithms are based on computing forwards and backwards approximations of the boundary, discontinuity and critical points. We explain how to handle the discontinuities in the symbolic dynamics which occur when the computed partition element boundaries are not disjoint. The method is applied to compute the symbolic dynamics and entropy bounds for the return map of the singular limit of a switching system with hysteresis and the forced Van der Pol equation.

© 2010 Elsevier B.V. All rights reserved.

1. Introduction

One-dimensional discrete time dynamical systems are widely used to describe physical and engineering systems in a simplified way, and often arise as return maps of continuous or hybrid systems of two dimensions. The dynamics of such systems can be complicated because even in one dimension the system can exhibit chaotic behaviour.

In this paper, we present some algorithms for computing the symbolic dynamics of one dimensional piecewise-continuous maps. Each of the algorithms constructs sofic shifts on the symbol space which over- and under-approximate the exact shift space of the maps. Further, the algorithms are designed to use interval methods, so can be rigorously implemented on a digital computer. Under certain nondegeneracy conditions the shift maps obtained converge to the exact symbolic dynamics as the precision is increased. The approximation of the symbolic dynamics allows us to also compute an arbitrary accurate approximation of the topological entropy of a map.

There has been considerable work on the symbolic dynamics of interval maps. A large class of results rely on the elementary fact that if there is a sequence of intervals $(I_n)_{n\in\mathbb{N}}$ such that $f(I_n) \supset I_{n+1}$ for all $n \in \mathbb{N}$, then there is a point x such that $f^n(x) \in I_n$ for all $n \in \mathbb{N}$. The celebrated theorem of Sharkovskii [1] on the coexistence of periodic orbits with different periods can be proved in this way, and stronger results can be obtained by considering the relative orderings of points forming finite invariant sets.

One of the most important contributions to one-dimensional dynamics is the kneading theory of Milnor and Thurston [2] for continuous multimodal maps. The theory gives necessary and sufficient conditions for an itinerary to be realised by an orbit in terms of the itineraries of the orbits of the critical points. The theory is most suited to and has received most attention for unimodal maps, since the itinerary of the critical point is sufficient to determine the symbolic dynamics. A more complete understanding of kneading theory for bimodal and trimodal maps was developed in [3,4]. Maps with discontinuities or holes were considered in [5]. The theory has been extended from interval maps to tree maps; see [6] for details.

Another motivation is related to a problem posed by Milnor on the computability of topological entropy [7]. The topological entropy of a continuous interval map is always lower-semicontinuous [8], and can be shown to be

* Corresponding author.
E-mail address: lorenzo.sella@cwi.nl (L. Sella).

0377-0427/$ – see front matter © 2010 Elsevier B.V. All rights reserved.
doi:10.1016/j.cam.2009.12.034

upper-semicontinuous in C^2 if the critical points are non-degenerate [9,10]. The constructions used in the proofs demonstrate that convergent approximations of the entropy can be effectively computed. In this paper we consider computability of symbolic dynamics, and convergence of the entropy of the generated shift space.

The main contributions of this paper are related to the practical implementation of the rigorous computation of symbolic dynamics based on the existing theory. Rather than start from a given periodic or invariant skeleton described combinatorially, we consider the computation of partition refinements, and compare the performance of different methods. We use rigorous interval arithmetics for the numeric computations, and show how to handle the difficulties which arise when extracting combinatorial data, including the use of references to store image and preimages, and how to resolve overlapping intervals. We also extend the kneading theory to be able to extract information about the dynamics from finite orbits, where the standard theory only considers infinite itineraries. We also consider the computation of symbolic dynamics relative to an arbitrary partition as opposed to the natural partition given by the critical points. A formal definition of the "effectively computable" symbolic dynamics is introduced, and an analysis of the convergence of the algorithms with respect to the theoretical restrictions on what is possible using numerical (as opposed to algebraic or symbolic) methods is also given.

A further motivation for this work was to obtain insight into the computation of symbolic dynamics which could be applied to higher-dimensional systems. For this reason, we do not only focus on methods based on kneading theory, which appear to be most powerful in one dimension, but also on methods based on backward iteration and covering relations, which are also applicable in higher dimensions.

The main mathematical techniques used in this article include interval analysis, symbolic dynamics, one-dimensional dynamical systems theory and kneading theory. Good references to these topics include the books [11–16]. Important standard references on kneading theory include [2,17–21,6]; other references include [4,5,22–25].

The paper is organised as follows. In Section 2, we give technical preliminaries on shift spaces symbolic dynamics, kneading theory and interval methods which we need later. In Section 3 we present algorithms for computing combinatorial mapping data, and extracting the symbolic dynamics using covering relations. In Section 4 we present methods for improving the symbolic dynamics obtained from the mapping data by considering kneading theory. In Section 5 we demonstrate the effectiveness of the method by applying it on several examples of continuous and discontinuous maps. In Section 6 we analyze two case studies of return maps of hybrid systems: an affine switching hybrid automaton and the singular limit of the Van Der Pol oscillator. Finally, in Section 7 we give some conclusions and suggestions for further research.

2. Theoretical preliminaries

We now introduce the basic definitions, terminology and results on symbolic dynamics and interval analysis which we will need.

2.1. Shift spaces and finite automata

We use $\vec{s}$ to denote the sequence $(s_0, s_1, s_2, \ldots)$. If A is a finite alphabet of symbols, recall that the sequence space $A^{\mathbb{N}}$ is compact under the *product topology* defined by the metric $d(\vec{s}, \vec{t}) = 2^{-m}$ where $m = \min\{n \in \mathbb{N} \mid s_n \neq t_n\}$. In other words, two sequences are "close" if they agree on a long prefix. The *shift map* σ on sequences A^{ω} is defined by $(\sigma\vec{s})_i = s_{i+1}$ for $i \in \mathbb{N}$. A *shift space* on A is a compact subset Σ of $A^{\mathbb{N}}$ which is invariant under σ. A shift Σ is a *subshift* of $\widehat{\Sigma}$ if $\Sigma \subset \widehat{\Sigma}$. If Σ is a subshift of $\widehat{\Sigma}$, then the shift map on $\widehat{\Sigma}$ simulates the shift map on Σ.

Since shift spaces are compact subsets of a metric space, we can measure the difference between two shift spaces using the Hausdorff distance. If Σ is a subshift of $\widehat{\Sigma}$, an alternative measure of the difference between Σ and $\widehat{\Sigma}$ is the difference in topological entropy h_{top}. The Hausdorff distance can be seen as a measure of the difference in the transient behaviour of two systems, whilst the entropy is a measure of the difference in the complexity of the recurrent behaviour.

A natural way of generating shift spaces is by finite automata. A *discrete automaton* is a tuple $\mathscr{A} = (Q, S, \delta, \omega)$ where Q is a finite sets, S is a (possibly infinite) set, $\delta : S \to \mathcal{P}(S)$ is the transition relation, and $\omega : S \to Q$ is the output map. An automaton is *finite* if S is finite. The dynamics generated by an automaton $\mathscr{A}$ is the set of all sequences $\vec{q} = (q_0, q_1, \ldots)$ such that there exist sequences $\vec{s} = (s_0, s_1, \ldots)$ such that $s_{i+1} \in \delta(s_i)$ and $\omega(s_i) = q_i$ for all i.

A shift is *sofic* if it is generated by a finite automaton. Since the set of sofic shifts is dense in the space of all shifts on an alphabet A, sofic shifts represented by finite automata are a convenient way of approximating arbitrary shifts.

2.2. Symbolic dynamics of piecewise-continuous maps

Symbolic dynamics is a powerful tool to analyse discrete-time dynamical systems. The basic idea is to compute the *itineraries* of orbits in terms of the regions of state space. The main complicating factor is that there is no nontrivial partition of a connected space M into compact pieces, so we instead use open sets whose closures cover the space.

A *topological partition* of a topological space X is a finite collection $\mathcal{P} = \{P_1, P_2, \ldots, P_k\}$ of mutually disjoint open sets such that $X = \bigcup_{i=1}^{k} \overline{P}_i$. It is convenient to assume that the elements of $\mathcal{P}$ are *regular* sets, that is, $\overline{P^{\circ}} = P$ for all $P \in \mathcal{P}$. The *boundary points* of $\mathcal{P}$ are elements of $\partial\mathcal{P} := \bigcup_{P\in\mathcal{P}} \partial P$. The *closure* of $\mathcal{P}$ is the collection $\overline{\mathcal{P}} = \{\overline{P}_1, \ldots, \overline{P}_k\}$. Given topological partitions $\mathcal{P}$ and $\mathcal{Q}$, we say that $\mathcal{Q}$ is a *refinement* of $\mathcal{P}$ if for all $Q \in \mathcal{Q}$, there exists $P \in \mathcal{P}$ such that $Q \subset P$. The *join* of $\mathcal{P}$ and $\mathcal{Q}$ is defined by $\mathcal{P} \vee \mathcal{Q} = \{P \cap Q \mid P \in \mathcal{P},\ Q \in \mathcal{Q} \text{ and } P \cap Q \neq \emptyset\}$.

We shall consider piecewise-continuous functions defined as follows:

Definition 1 (*Piecewise-Continuous Map*). A function $f : X \to X$ is *piecewise-continuous* if there is a topological partition $\mathcal{P}$ of X such that for all $P \in \mathcal{P}$, $f|_P$ is continuous, and that $f_P := f|_P$ extends to a continuous function $\bar{f}_P$ on $\overline{P}$. We say that f is $\mathcal{P}$-*continuous*. We let $f^\circ = f|_{\bigcup \mathcal{P}}$, and define $\bar{f}$ by $\bar{f}(x) = \bigcup\{\bar{f}_P(x) \mid x \in \overline{P}\}$.

Given a topological partition, we can define the symbolic dynamics of a piecewise-continuous function f.

Definition 2 (*Symbolic Dynamics*). Let $f : X \to X$ be a piecewise-continuous map and $\mathcal{Q}$ be a topological partition of X.

- The *inner symbolic dynamics* of f, denoted $\Sigma(f, \mathcal{Q})$, is the closure of the set of all $\mathcal{Q}$-itineraries of orbits of f°.
- The *outer symbolic dynamics* of f, denoted $\Sigma(f, \overline{\mathcal{Q}})$, is the set of all $\overline{\mathcal{Q}}$-itineraries of orbits of $\bar{f}$.

The motivation for these definitions are that the inner and outer symbolic dynamics give under and over approximations of the symbolic dynamics which can be effectively computed. We shall return to these definitions in Section 2.3. We shall then see that the outer symbolic dynamics may give a "bad" approximation in the differentiable case, and consider ways of improving the situation.

The following results are trivial, but provide the main tools for determining whether an itinerary is present in the system.

Proposition 1. *If there is an orbit $\vec{x}$ of $\bar{f}$ such that $x_i \in \overline{R}_i$ with $\overline{R}_i \subset \overline{P}_i$ for all i, then $\bar{f}_{P_i}(\overline{R}_i) \cap \overline{R}_{i+1} \neq \emptyset$ for all i.*

Proposition 2. *Suppose $n \in \mathbb{N} \cup \{\infty\}$ and $(R_0, R_1, \ldots)$ is a sequence such that $f(R_i) \supset R_{i+1}$ for all $i < n$, and $f(R_i) \subset R_{i+1}$ for all $i \geq n$. Then there is an orbit $(x_0, x_1, \ldots)$ of f such that $x_i \in R_i$ for all i.*

The following result relates the inner and outer symbolic dynamics.

Theorem 1. *If the sets $\overline{Q}$ for $Q \in \mathcal{Q}$ are compact, then the inner symbolic dynamics of f is a subshift of the outer symbolic dynamics of f.*

2.3. One-dimensional dynamical systems

Symbolic dynamics for one-dimensional maps is substantially easier than in higher dimensions. The partition elements $Q \subset \mathcal{Q}$ are intervals, so can easily be represented by their boundary points q_i. Of particular importance are the *monotone branches*, sometimes known as *laps*. It is trivial that any point has at most one preimage in any lap, and this point is readily computed by bisection.

Let I be an interval, an interval map $f : I \to I$ is *piecewise-monotone-continuous* if there is a topological partition $\mathcal{L}$ of I into intervals such that $f|_L$ is monotone and continuous on each $L \in \mathcal{L}$. We say that f is $\mathcal{L}$-monotone-continuous. Note that if f is $\mathcal{L}$-monotone-continuous, then f is also $\mathcal{L}'$-monotone-continuous for any refinement $\mathcal{L}'$ of $\mathcal{L}$.

If f is $\mathcal{P}$-continuous, with $\partial\mathcal{P} = \{p_0, p_1, \ldots, p_k\}$, then we let $D^\pm = \{p_0^+, p_1^-, p_2^+, \ldots, p_{k-1}^-, p_k^+\}$, the set of discontinuities of f We let C be the set of critical points of f.

Assumption 1. In this paper, we shall henceforth assume that our system is described by a piecewise-monotone-continuous function. We also assume that the number of discontinuity and critical points is known, and that these can all be computed to an arbitrary accuracy.

Within the class of piecewise-monotone-continuous functions, we can consider locally-uniform perturbations by functions with the same critical and discontinuity points. This gives a refined notion of approximations of the symbolic dynamics within a class.

Definition 3 (*Symbolic Dynamics*). Let $\mathcal{Q}$ be a topological partition, and $\mathcal{L}$ a refinement of $\mathcal{Q}$. Suppose $f : X \to X$ is monotone continuous on each element of $\mathcal{L}$.

- The *lower symbolic dynamics* $\underline{\Sigma}(f, \mathcal{Q})$ of f is the closure of the set of all sequences $\vec{s}$ such that there exists $\epsilon > 0$ such that for all ϵ-perturbations f_ϵ of f which are $\mathcal{L}$-monotone-continuous, f_ϵ has an orbit with $\mathcal{Q}$-itinerary $\vec{s}$.
- The *upper symbolic dynamics* $\overline{\Sigma}(f, \mathcal{Q})$ of f is the set of all sequences $\vec{s}$ such that for all $\epsilon > 0$, there exists an ϵ-perturbation f_ϵ of f which is $\mathcal{L}$-monotone-continuous and has an orbit with $\mathcal{Q}$-itinerary $\vec{s}$.

If $\mathcal{Q}$ is a topological partition with boundary points $\{q_0, q_1, \ldots, q_m\}$ and elements $Q_k = (q_k, q_{k+1})$, then we introduce new symbols $\binom{0}{1}, \binom{1}{2}$ etc. as the code for the points $q_0, q_1, \ldots$. In other words, we use the symbol $\binom{1}{2}$ for a point in $\overline{Q}_1 \cap \overline{Q}_2$. This greatly facilitates the writing of itineraries. We also write $\mathrm{itin}(x^\pm) = \lim_{\epsilon \to 0} \mathrm{itin}(x \pm \epsilon)$.

The following example shows that the upper symbolic dynamics for maps with the same monotone branches can be different from the outer symbolic dynamics.

Example 1. Let $X = [-1, 1]$ and $f(x) = x/2$. Let $\mathcal{Q} = \{Q_0, Q_1\}$ with $Q_0 = (-1, 0)$ and $Q_1 = (0, 1)$.

Since any sequence of zeroes and ones is a valid itinerary of the point 0, the outer symbolic dynamics are the full shift on $\{0, 1\}$. Further, among all perturbations of f, we can generate orbits with all itineraries by fitting a small version of the tent map near 0.

For perturbations f_ϵ of f among monotone maps (which include all C^1-perturbations), the possible itineraries depend on whether $f_\epsilon(0) \gtrless 0$. For $f_\epsilon(0) > 0$, there exists N such that the $\mathcal{Q}$-itineraries are of the form $0^n\overline{1}$ for $n \leq N$, and for $f_\epsilon(0) < 0$

we have itineraries $1^n\overline{0}$ for $n \leq N$. For $f_\epsilon(0) = 0$, the $\mathcal{Q}$-itineraries are $\overline{0}$ and $\overline{1}$. Taking the size of the perturbation to be zero, we obtain upper symbolic dynamics $\{0^n\overline{1},\ 1^n\overline{0} \mid n = 0, 1, \ldots\}$. The inner and lower symbolic dynamics are both $\{\overline{0}, \overline{1}\}$.

In general, it is possible to show that the upper symbolic dynamics are a subset of the outer symbolic dynamics, and that the outer symbolic dynamics can be obtained by removing the restriction that the perturbations f_ϵ must have the same laps as f.

2.4. Kneading theory

The original kneading theory was developed for multimodal maps in [2]. The theory was extended to maps of the interval with "holes" in [5,23], which have a similar flavour to discontinuous maps. In this section we give a review of the kneading theory for multimodal maps without discontinuities. Rather than use Milnor and Thurston's approach using formal power series and a kneading matrix, we will work with itineraries and covering relations, since this is simpler and ties in better with the computation of sofic shifts.

Let f be a multimodal map defined on the interval $I = [a, b]$ with critical points $c_1, \ldots, c_{l-1}$. Let $L_j = [c_{j-1}, c_j]$ for $j = 1, \ldots, l$, where we take $c_0 = a$ and $c_l = b$. For $j \in \{1, \ldots, l\}$, let ε_j be equal to $+1$ if f is increasing over the interval I_j, and -1 if f is decreasing over L_j. For a sequence $\vec{s} \in \{1, \ldots, l\}^{\mathbb{N}}$, denote by $\varepsilon_{\vec{s},j}$ or $\varepsilon_{s_0,s_1,\ldots,s_{s-1}}$ the product $\varepsilon_{s_0}, \varepsilon_{s_1}, \ldots, \varepsilon_{s_{j-1}}$.

We define an ordering on the itineraries of f. Suppose $\vec{s}$ and $\vec{t}$ are sequences, and $j = \min\{i | s_i \neq t_i\}$, and suppose $s_j < t_j$. Then $\vec{s} < \vec{t}$ if, and only if, $\varepsilon\, s_j < \varepsilon\, t_j$, where $\varepsilon = \varepsilon_{\vec{s},j} = \varepsilon_{\vec{t},j}$.

We now consider whether there exists an orbit with a given itinerary. Suppose the itineraries of the images of the critical points $c_1, \ldots, c_{l-1}$ are $\vec{k}_j$, that is $\vec{k}_j = \mathrm{itin}(f(c_j))$. Suppose $\vec{t}$ is the itinerary of a point x. Then if $c_i < x < c_{i+1}$, then either $f(c_i) < f(x) < f(c_{i+1})$ or $f(c_{i+i}) < f(x) < f(c_i)$ depending on whether f is increasing or decreasing over (c_i, c_{i+1}). Since $\mathrm{itin}(f(x))$ is $\sigma(\mathrm{itin}(x))$, where $\mathrm{itin}(x)$ is the itinerary of x. We deduce that $\vec{t}$ is an itinerary if and only if $\sigma^{n+1}(\vec{t}) \in [\vec{k}_{t_n}, \vec{k}_{t_n+1}]$, where the endpoints of the interval may be reversed. We may also consider the endpoints of the intervals.

We have the following result.

Theorem 2. *Let $\vec{s}$ be a sequence in $\{1, \ldots, l\}^{\mathbb{N}}$. Then $\vec{s}$ is the itinerary of an orbit $\vec{x}$ of f if $\sigma^{n+1}(\vec{s})$ lies between $\vec{k}_{s_n-1}$ and $\vec{k}_{s_n}$ for all n, where $\vec{k}_j$ is the itinerary of $f(c_j)$.*

In the unimodal case, we have $f(a) = f(b) = a$, and $\iota(a) = (0, 0, \ldots)$. Hence we obtain the classical result that $\vec{s}$ is an itinerary of a point x if, and only if $\sigma^{n+1}(\vec{s}) \leq \vec{k}$ for all n, where $\vec{k}$ is the itinerary of $f(c)$, the image of the critical point.

2.5. Computability theory and numerical computation

Since we typically cannot compute an arbitrary piecewise-continuous map, such as the return map of a hybrid system, exactly, we resort to numerical approximation. In order to ensure that we can obtain rigorous conclusions from approximate numerics, we compute error bounds for all quantities. Hence a numerical approximation of a real number x is represented by an interval $[\underline{x}, \overline{x}]$ such that $\underline{x} \leq x \leq \overline{x}$. We henceforth use the notation $\lfloor x \rceil$ for an interval approximation of x, and $\underline{x}, \overline{x}$ for the lower and upper bounds on x. We let $\mathbb{I}$ denote the set of all rational intervals i.e. $\mathbb{I} = \{(a, b) \mid a, b \in \mathbb{Q}\}$.

In the theory of effective (Turing) computability over the reals, we represent a real number as a sequence of approximations, either as floating points x_n with n binary digits of accuracy, or as a convergent sequence of intervals. In this representation, all arithmetical operations are computable, but comparison tests are only *semidecidable* rather than being decidable. For if real numbers x and y differ, then we can determine $x < y$ or $x > y$ in finite time. If, however, $x = y$, then even if we know both x and y up to n bits, we can still never know that indeed $x = y$. This means that any algorithm which tests for an (in)equality will not terminate on some inputs. In practice, we can replace the standard comparison operator on reals with an extended comparison operator, so that $\mathrm{cmp}_\epsilon(x, y)$ may (nondeterministically) return indeterminate value $\uparrow$ if $|x-y| < \epsilon$.

When using interval arithmetic, we can test for an equality, but the result can only be true if both intervals are singletons. If $\lfloor x \rceil$, $\lfloor y \rceil$ and $\lfloor z \rceil$ overlap, then we cannot say anything about the relative ordering of x, y and z, it is even possible that all three values are equal. If, however, $\lfloor y \rceil$ overlaps both $\lfloor x \rceil$ and $\lfloor z \rceil$, but $\lfloor x \rceil < \lfloor z \rceil$, then the only possible orderings are $y < x < z, x = y < z, x < y < z, x < y = z$ and $x < z < y$. Further, by increasing the precision, we can eventually compute $\lfloor y \rceil$ sufficiently accurately so that either $\lfloor y \rceil > \lfloor x \rceil$ or $\lfloor y \rceil < \lfloor z \rceil$, reducing the possible relative orderings.

More generally, we say that intervals $\lfloor y_0 \rceil, \ldots, \lfloor y_k \rceil$ form a *chain* if $\lfloor y_{i-1} \rceil$ overlaps $\lfloor y_i \rceil$ for $i = 1, \ldots, k$, but $\lfloor y_0 \rceil < \lfloor y_k \rceil$. In this case, increasing the precision of computation, and hence the accuracy of the interval approximations, will eventually partition the intervals so that (possibly after a reordering) there exists m such that $\lfloor i \rceil < \lfloor j \rceil$ whenever $i \leq m < j$. We say intervals $\lfloor y_1 \rceil, \ldots, \lfloor y_k \rceil$ form a *cluster* if $\lfloor y_i \rceil$ intersects $\lfloor y_j \rceil$ for all $i, j = 1, \ldots, k$. Given a finite set of points with interval bounds, we can always partition the points into clusters by increasing the precision.

In order to work with continuous functions, we assume that given an interval approximation $\lfloor x \rceil$ of x, we can effectively compute an approximation $\lfloor y \rceil$ of $f(x)$. This is formulated by the notion of *interval extension*.

Definition 4 (*Interval Extension*). Let f be a continuous interval map. Then an *interval extension* of f is a function $\lfloor f \rceil : \mathbb{I} \to \mathbb{I}$ such that

1. $f(\lfloor x \rceil) \subset \lfloor f \rceil(\lfloor x \rceil)$ for all $\lfloor x \rceil \in \mathbb{I}$,

2. if $\lfloor x \rceil \subset \lfloor y \rceil$, then $\lfloor f \rceil(\lfloor x \rceil) \subset \lfloor f \rceil(\lfloor y \rceil)$, and
3. if $\bigcap_{i=1}^{\infty} \lfloor x_n \rceil = \{x\}$, then $\bigcap_{i=1}^{\infty} \lfloor f \rceil(\lfloor x_n \rceil) = \{f(x)\}$.

If f is n-times continuously-differentiable, we also assume that an interval extension is available for derivatives $f^{(i)}(x)$ for $i = 1, \ldots, n$.

Definition 5 (*Representation of Piecewise-Continuous Functions*). Let f be a $\mathcal{P}$-continuous interval map. An interval extension f consists of

1. an enumeration of each partition element $P_i \in \mathcal{P}$, and
2. an interval extension of each piece f_i over the closure of P_i.

Note that from the data given, we can compute approximations of the discontinuity points, since a point d lies on the boundary of two partition elements if and only if, for all intervals $J \ni d$, there exist $\bar{I}_{i_1} \subset P_{i_1}$ and $\bar{I}_{i_2} \subset P_{i_2}$ such that $J \cap I_{i_1} \neq \emptyset$ and $J \cap I_{i_2} \neq \emptyset$.

In practice, we combine numerical and symbolic approaches. For example, in the unimodal map $x \mapsto \mu x(1-x)$, we know that $f(0) = f(1) = 0$ and that $f'(1/2) = 0$. Letting $a = 0$, $b = 1$ and $c = 1/2$, we know exactly that $b \mapsto a \mapsto a$ and that c is a critical point.

We may sometimes want to *define* boundary points of the partition $\mathcal{Q}$ as fixed, periodic or critical points. For example, if we want to use the period-two orbit (q_1, q_2) of the unimodal map at $\mu = 3.92$ with negative derivative as partition boundary elements, we can define the position of q numerically by $\lfloor q_1 \rceil = [0.356, 0.357]$ and $\lfloor q_2 \rceil = [0.898, 0.899]$ and symbolic images $q_1 \mapsto q_2 \mapsto q_1$.

3. Computing symbolic dynamics using covering relations

We will consider the computation of symbolic dynamics for a $\mathcal{P}$-continuous map f with respect to the partition $\mathcal{Q}$. We let B be the boundary points of $\mathcal{Q}$, C the critical points of f and D the discontinuity points of f.

Our basic strategy for computing symbolic dynamics is as follows

Algorithm 1. 1. Compute the topological partition $\mathcal{L}$ such that f is monotone and continuous on each piece of $\mathcal{L}$
2. Refine the partition $\mathcal{L} \vee \mathcal{Q}$ to obtain a partition $\mathcal{R}$.
3. On the refined partition $\mathcal{R}$, compute the symbolic dynamics by considering covering relations $f(R) \supset R', f(R) \subset R'$ and $f(R) \cap R' \neq \emptyset$.

There are a number of difficulties which arise when actually trying to implement this strategy. The first is that the discontinuity and critical points may be difficult to locate exactly, and we need to use approximations. This can be the case even if we are given the map in explicit form. A second difficulty is that there are many ways of refining the partition, and we need to find ways which give good approximations of the dynamics with as little computational effort possible. A third difficulty is that the boundary points of the refined partition may be difficult to compute exactly, and even the relative ordering of the boundary points on the interval may be difficult to compute. Finally, the basic method of extracting symbolic dynamics using covering relations can be quite crude, and it is often useful to improve the results by using kneading theory.

3.1. Mapping data

In order to refine the partition, we need to add extra points to the partition and determine their images and/or preimages. In general, given a point p, we will not be able to compute its image $q = f(p)$ arbitrarily accurately, so we generally need to represent points by intervals $q \in \lfloor q \rceil$. However, since $\lfloor q \rceil$ is an interval containing $f(p)$, we do know that $f(p) \in \lfloor q \rceil$. Similarly, computing the image $r = f(q) = f^2(p)$, we obtain the interval $\lfloor r \rceil \supset f(\lfloor q \rceil)$, though we know that $\lfloor r \rceil$ is an interval containing the exact image r of the point $q \in \lfloor q \rceil$.

The data we can compute about our function will therefore consist of a finite set of points, for which we know the image map exactly, but know the value of the points only approximately. We formalise this notion as a *mapping dataset* for the function.

Definition 6. A *mapping dataset* $\mathcal{F}$ consists of a finite set Y of point labels, together with

1. an *image* function $\rightsquigarrow: Y' \to Y$, and
2. a *value* function $\lfloor \cdot \rceil : Y \to \mathbb{I}$.

We alternatively write $f(x) = y$ if $x \rightsquigarrow y$. From the interval values we can deduce

3. a partial ordering $\leq$ on Y, defined by $x \leq y \iff \lfloor x \rceil \leq \lfloor y \rceil$ (by which we mean $\overline{x} \leq \underline{y}$).

Further, there is a finite totally ordered subset Z of Y such that if $z_i \leq x \leq y \leq z_{i+1}$, then either $f(z_i) \leq f(x) \leq f(y) \leq f(z_{i+1})$ or $f(z_{i+1}) \leq f(y) \leq f(x) \leq f(z_i)$. The points of Z correspond to the critical points c_i and discontinuity points $d_i^{\pm}$.

The data type representing a point y therefore has two fields, a `value` field which is (an approximation of) the numerical value of y, and a `image` field which is a reference or pointer to the object representing $f(y)$. If $f(y)$ has not been computed, then the image field is `null`. If d is a discontinuity point, then we store two image points, namely the image of d under both branches of $\bar{f}$ at d, which we denote $f(d^-)$ and $f(d^+)$.

In the case that we can compute images and/or preimages exactly, then the value field of each point is an exact real number, the resulting mapping dataset is totally ordered, and the complement of the set Y forms a topological partition. Otherwise, we cannot extract a topological partition from the mapping data set, but instead obtain a topological partition for each linear order compatible with the mapping dataset. We can assume that the ordering is *clustered*, which means that if $w < y$, then for all x, either $w < x$ or $x < y$. If these interval values are disjoint, so $\lfloor x \rceil \gtrless \lfloor y \rceil$ if $x \neq y$, then we can recover a topological partition.

To compute the critical points numerically, we need information on the derivative f. A point c is a critical point if $f'(c) = 0$, and the zeros of f' can easily be computed to arbitrary accuracy by a bisection strategy. In certain degenerate cases, we may not be able to distinguish two discontinuity points of f, or a discontinuity point and a critical point. Although it is possible to handle these cases in a consistent way, in this paper we assume for simplicity that these cases do not arise.

3.2. Partition refinement strategies

In this section, we give the basic refinement strategies used.

Definition 7. Let $\mathcal{Q}$ be the initial partition and $\mathcal{L}$ the partition into monotone branches. The forward-refinement partition at step n is the partition whose end points are $Y = \partial\mathcal{Q} \cup \bigcup_{z\in\partial\mathcal{L}}\{f^j(z_i) \mid j = 0, \ldots, n\}$.

Definition 8. Let $\mathcal{Q}$ be the initial partition and let $\mathcal{P}$ be the partition into continuous branches. The backward-refinement partition at step n is the partition whose end points are $Y = \bigcup_{z\in\partial\mathcal{P}\cup\partial\mathcal{Q}}\{f^{-j}(z) \mid j = 0, \ldots, n\}$.

The forward refinement of a partition $\mathcal{R}$ can be easily computed, since we need simply to compute the images of all boundary points of $\mathcal{R}$. To compute the backward refinement of $\mathcal{R}$ we need to compute preimages of $r \in \partial\mathcal{R}$. Since f is strictly monotone on each element of $\mathcal{L}$, so we can use a bisection strategy to locate the preimage of y in each $L \in \mathcal{L}$, which must be unique (if it exists).

The advantage of the forward refinement strategy is that better results can usually be obtained with fewer partition points, since the growth of the number of endpoints is linear in the number of steps. The advantage of backward refinement is that each partition element of an n-step backward refinement of $\mathcal{Q}$ determines the first n elements of a $\mathcal{Q}$-itinerary. Define sets $Q_{i_0,i_1,\ldots,i_{n-1}}$ recursively by $Q_{i_0} \in \mathcal{Q}$ and $Q_{i_0,i_1,\ldots,i_{n-1}} = Q_{i_0} \cap f^{-1}(Q_{i_1,\ldots,i_{n-1}})$. Then it is easy to see that $Q_{i_0.i_1.\ldots.i_{n-1}} = \{\vec{y} \mid f^k(\vec{y}) \in Q_{i_k} \text{ for } k = 0, \ldots, n-1\}$. Further, the endpoints of $Q_{i_0,i_1,\ldots,i_{n-1},i_n}$ are points in $f^{-n}(B \cup D)$.

The following partition refinement strategy attempts to combine the efficiency of forward refinement with the better theoretical properties of backward refinement.

Definition 9. Let $\mathcal{Q}$ be the initial partition, let $\mathcal{L}$ be the partition into monotone branches, and $\mathcal{R}_0 = \mathcal{Q} \vee \mathcal{L}$. The forward-looking backward-refinement partition at step n is the partition $\mathcal{R}_n$ whose end points are

$$\left\{p \in f^{-1}(\partial\mathcal{R}_{n-1}) \mid \exists q \in \partial\mathcal{R}_{n-1} : f^{-1}(\partial\mathcal{R}_{n-1}) \cap \operatorname{conv}\{p, f(q)\} = \{p\}\right\}.$$

In other words, among all preimages up to order m of endpoints of the initial partition, this refinement considers only the ones which are the closest to at least one endpoint of the initial partition, in this way we minimize the size of elements of the partition which do not cover exactly other elements of the partition, and consequently the gap between lower and upper symbolic dynamics.

The above strategy gives a growth of end points which is linear with the number of steps and both lower and upper approximation converge monotonically.

Despite this great improvement an algorithm using the latest strategy also has an exponential running time in the number of steps because it still requires us to compute the preimages which grow exponentially in the number of steps. The only algorithm which has a linear running time and converges to the symbolic dynamics is the one using the kneading theory as will be explained in Section 4.

3.3. Eventually periodic discontinuity and critical points

Suppose that the backward images of the partition boundary points are all disjoint from each other, and disjoint from the critical and discontinuity points. Then the partitions computed using backward refinement are all disjoint, and so can be ordered, given enough information about the function. However, it may be the case that certain preimages intersect, or are equal to critical or discontinuity points, and in this case they cannot be ordered. Similarly, if the forward images of critical or discontinuity points are not all disjoint, or touch partition boundary points, then we lose the ability to order them.

In some cases, we may be able to use algebraic information about the function to prove equality. For example, if we know that a partition boundary is also a fixed point, then we can set the image explicitly, rather than use approximations. The symbolic dynamics are discontinuous at a point for which $f^n(c) = q$, since we introduce the possibility of a new transition after n steps.

During our interval computations, we will find cases for which (say) $f^n(c) \approx_\epsilon q$ for a partition boundary point q. If this is the case, we do not know whether $f^n(c) < q, f^n(c) > q$ or $f^n(c) = q$, though we do know that in either of the former two possibilities, increasing the precision will eventually give the correct answer. In order to study this situation, we continue iterating the interval. Note that if $\lfloor x \rceil$ and $\lfloor y \rceil$ overlap, then so do $\lfloor f(x) \rceil$ and $\lfloor f(y) \rceil$, and therefore $\lfloor f \rceil(\lfloor x \rceil)$ and $\lfloor f \rceil(\lfloor y \rceil)$.

Upon further computation, we may find a case in which an interval $\lfloor y \rceil$ intersects two disjoint intervals $\lfloor x \rceil$ and $\lfloor z \rceil$. In this case, we increase the precision until $\lfloor y \rceil$ is disjoint from either $\lfloor x \rceil$ or $\lfloor z \rceil$.

To resolve the overlap, we consider the dynamics for the three cases $x < y$, $x = y$ and $x > y$. In the case of equality, we can combine the exact orbits. In the case of inequality, suppose that y is not a critical or discontinuity point, then we know the monotone branch that y lies in, and hence the relative ordering of $f^i(x)$ and $f^i(y)$ for as long as these have been computed.

If there are multiple overlaps, then we need to consider all possible orderings. In principle, this can be very expensive, but in practice the condition that the algorithm increases the precision if we find a chain of overlaps means that the number of combinations remains small (at most l overlaps, where l is the number of laps).

3.4. Covering relations

The simplest way to extract symbolic dynamics is directly via covering relations. Given a partition $\mathcal{R}$ and covering relations between its elements we want to construct sofic shifts under- and over-approximating the symbolic dynamics. Let $\mathcal{L}$ be the partition into monotone branches, and $\mathcal{R}_0 = \mathcal{Q} \vee \mathcal{L}$.

Definition 10. Let $f : X \to X$ be a $\mathcal{P}$-continuous map and $\mathcal{Q}$ a partition of X. Let $\mathcal{L}$ be the partition of X into monotone branches of f and let $\mathcal{R} = \mathcal{Q} \vee \mathcal{L}$.

Define *covering relations* relations $R \longrightarrow R'$ and $R- \to R'$ on $\mathcal{R} \times \mathcal{R}$ by $R \longrightarrow R'$ if $f(R) \supset R'$ and $R- \to R'$ if $f(R) \cap R' \neq \emptyset$.

We define the *attracting subset* $\mathcal{A} \subset \mathcal{R}$ to be the maximal subset of $\mathcal{R}$ such that for all $A \in \mathcal{A}$, there exists $A' \in \mathcal{A}$ such that $f(A) \subset A'$. Define relation $\hookrightarrow$ by $A \hookrightarrow A'$ if $f(A) \subset A'$.

We define a *lower symbolic dynamics* $\underline{\Sigma}(f, \mathcal{Q}, \mathcal{R})$ to be determined by the transitions $\longrightarrow$ and $\hookrightarrow$, and *upper symbolic dynamics* $\overline{\Sigma}(f, \mathcal{Q}, \mathcal{R})$ by the transitions $- \to$.

We can represent the symbolic dynamics visually by a graph with vertices $\mathcal{R}$, each vertex R being labelled with the element $Q \in \mathcal{Q}$ with $R \subset Q$, and edges $- \to$, $\longrightarrow$ or $\hookrightarrow$ determined by the transition relations.

It is clear that the lower symbolic dynamics are an under-approximation of the inner symbolic dynamics, $\underline{\Sigma}(f, \mathcal{Q}, \mathcal{R}) \subset \underline{\Sigma}(f, \mathcal{Q})$, and the upper symbolic dynamics are an over-approximation of the inner symbolic dynamics, $\overline{\Sigma}(f, \mathcal{Q}, \mathcal{R}) \supset \underline{\Sigma}(f, \mathcal{Q})$.

However, we may not have $\overline{\Sigma}(f, \mathcal{Q}, \mathcal{R}) \supset \overline{\Sigma}(f, \mathcal{Q})$ due to problems with the endpoints of partition elements. For example, if c is a critical point and $f(c) \in \{r\} = R_i \cap R_{i+1}$, then we should allow broken arrows from each interval containing c to R_i and R_{i+1} to obtain an over-approximation of the upper symbolic dynamics. If exact mapping data is available, we can augment the graph with vertices $z \in B \cup C \cup D^{\pm}$ with the appropriate labelling and arrows.

In order to determine the transitions $R \longrightarrow R'$ and $R- \to R'$, we need to know the relative ordering of the boundary points i.e. whether $r_i < r_j$, $r_i = r_j$ or $r_i > r_j$, and the image point r_k of r_i under f. As long as the interval approximations of the boundary points of $\mathcal{R}$ do not overlap, we can determine the relative ordering by taking a sufficiently high precision. However, if the boundary points do overlap, then there is more than one topological partition consistent with the mapping data.

In order to obtain under- and over-approximations of the symbolic dynamics, we consider *all* possible topological partitions consistent with the mapping data. Note that knowledge of the monotone branches of f may help reduce the number of possibilities. For example, if the numerical values of r_i and r_j overlap, then we need to consider partitions with $r_i < r_j$, $r_i = r_j$ and $r_i > r_j$. However, if r_i, r_j lie in an increasing branch, then $f(r_i) \gtrless f(r_j)$ according to $r_i \gtrless r_j$. We can also dispense with the case $r_i = r_j$, since this will always provide better approximations than the cases $r_i \neq r_j$. We therefore only need to consider two cases if $\lfloor r_i \rceil$ and $\lfloor r_j \rceil$ overlap.

We therefore have the following algorithm for computing over- and under-approximations of the symbolic dynamics from a mapping dataset $\mathcal{F}$.

Algorithm 2.
1. Compute the set of all partitions $\mathcal{R}$ consistent with the mapping dataset $\mathcal{F}$ and for which there is no equality in uncertain comparisons.
2. On each refined partition $\mathcal{R}$, compute lower and upper symbolic dynamics $\underline{\Sigma}(f, \mathcal{Q}, \mathcal{R})$ and $\overline{\Sigma}(f, \mathcal{Q}, \mathcal{R})$.
3. Let the lower symbolic dynamics $\Lambda = \underline{\Sigma}(f, \mathcal{Q}, \mathcal{F})$ be the intersection of all $\underline{\Sigma}(f, \mathcal{Q}, \mathcal{R})$ with $\mathcal{R}$ consistent with $\mathcal{F}$, and the upper symbolic dynamics $\Upsilon = \overline{\Sigma}(f, \mathcal{Q}, \mathcal{F})$ be the union of all $\overline{\Sigma}(f, \mathcal{Q}, \mathcal{R})$ with $\mathcal{R}$ consistent with $\mathcal{F}$.

It is clear that Λ is a subshift of $\underline{\Sigma}(f, \mathcal{Q})$, and Υ is a supershift of $\underline{\Sigma}(f, \mathcal{Q})$. In Section 3.6 we shall see that the symbolic dynamics converges to the upper and lower symbolic dynamics of f, and that this convergence is monotone using backward refinement.

3.5. Combining intervals

The dynamics obtained using covering relations can be improved by *combining intervals*. The motivation for this trick is as follows. Suppose I_1 and I_2 are adjacent intervals, and $I_1 \cap I_2$ is a point x with no computed image under f. Then we can make a new formal symbol I_{12} which covers any interval covered by $I_1 \cup I_2$. Whenever an interval J covers I_1 and I_2, we replace the arrows $J \longrightarrow I_1$ and $J \longrightarrow I_2$ with $J \longrightarrow I_{12}$. Whenever an interval K is covered by $I_1 \cup I_2$, we add an arrow $I_{12} \to K$.

The resulting symbolic dynamics are a supershift of the previous dynamics, since any sequence passing $J \longrightarrow I_i \rightarrow K$ for $i = 1, 2$ either remains as is, or is changed to $J \longrightarrow I_{12} \longrightarrow K$.

We formalise the conditions on the combined intervals as follows.

Definition 11. Let $\mathcal{I} \supset \mathcal{R}$ be a collection of intervals such that every $I \in \mathcal{I}$ is contained in some $L \in \mathcal{L}$ and has endpoints in $\partial\mathcal{R}$. Define relations $\longrightarrow$, and $- \rightarrow$ satisfying:

1. If $f(I) \supset J$, then there exists $K \supset J$ such that $I \longrightarrow K$.
2. If $f(I) \cap J \neq \emptyset$, then there exists $K \subset J$ such that $I - \rightarrow K$.
3. If $I \longrightarrow J$, then $f(I) \supset J$.
4. If $I - \rightarrow J$ and $K \subset J$, then $f(I) \cap K \neq \emptyset$.
5. If $I - \rightarrow J$ and $I - \rightarrow K$ or $I \longrightarrow J$ and $I \longrightarrow K$, then $J \cap K = \emptyset$.

Condition 5 ensures that every orbit is assigned a unique itinerary.

The next result shows that the symbolic dynamics computed using combined intervals improves on those computed directly.

Theorem 3. *Let Λ and Υ be the lower and upper shifts defined by the partition $\mathcal{R}$, and Λ' and Υ' defined by the relations $\longrightarrow$ and $- \rightarrow$ on $\mathcal{I}$. Then $\Lambda \subset \Lambda' \subset \underline{\Sigma}(f, \mathcal{Q}) \subset \Upsilon' \subset \Upsilon$.*

Proof. Any $\mathcal{Q}$-itinerary $\vec{s}$ in Λ is also in Λ': Take a sequence $\vec{R}$ with $R_i \subset Q_i$ and $f(R_i) \supset R_{i+1}$. Define $I_0 = R_0$, and I_{i+1} recursively such that $R_{i+1} \subset I_{i+1}$ and $I_i \longrightarrow I_{i+1}$. The resulting sequence $\vec{I}$ shows that $\vec{s}$ is in Λ'.

Any $\mathcal{Q}$-itinerary in Λ' also is an itinerary of f: If $I_i \longrightarrow I_{i+1}$ in the shift Λ', then $f(I_i) \supset I_{i+1}$.

Any $\mathcal{Q}$-itinerary of f is also in Υ': If $\vec{x}$ is an orbit with itinerary $\vec{s}$ with $x_i \in R_i$ for $R_i \in \mathcal{R}$, we can choose $I_0 \supset R_0$ and then recursively find I_{i+1} such that $I_{i+1} \supset R_{i+1}$ and $I_i - \rightarrow I_{i+1}$ since $f(I_i) \cap R_{i+1} \neq \emptyset$.

Any $\mathcal{Q}$-itinerary in Υ' is also in Υ: Suppose $I_i - \rightarrow I_{i+1}$ for all $i \in \mathbb{N}$. Suppose $R_j \in \mathcal{R}$ with $R_j \subset I_j$. Then $f(I_{j-1}) \cap R_j \neq \emptyset$, so there exists $R_{j-1} \subset I_{j-1}$ with $f(R_{j-1}) \cap R_j \neq \emptyset$. □

3.6. Convergence to the symbolic dynamics

We now describe how the sofic shifts computed by Algorithm 1 approximate the symbolic dynamics of f, and give sufficient conditions under which the approximations converge.

We first consider monotonicity of the computed shift dynamics.

Theorem 4. *Suppose f is a $\mathcal{P}$-monotone-continuous map, $\mathcal{Q}$ is a topological partition, that $\mathcal{R}_1$ is a refinement of $\mathcal{P} \vee \mathcal{Q}$ and $\mathcal{R}_2$ a refinement of $\mathcal{R}_1$. Then the over-approximation of the $\mathcal{Q}$-itineraries of f induced by $\mathcal{R}_2$ is a subset of the set of $\mathcal{Q}$-itineraries induced by $\mathcal{R}_1$.*

Proof. Suppose $I, J \in \mathcal{R}_1$, $K, L \in \mathcal{R}_2$, $I \subset K$ and $J \subset L$. Then if $f(K) \cap L \neq \emptyset$ we have also $f(I) \cap J \neq \emptyset$. Hence if there is a broken arrow from K to L, there is also a broken arrow from I to J. The result follows. □

When using forward refinement it is not necessarily true that the topological entropy of the finite-type shift generated by $\mathcal{R}_2$ is lower than that of the finite-type shift generated by $\mathcal{R}_1$.

Theorem 5. *Suppose f is a $\mathcal{P}$-monotone-continuous map, $\mathcal{Q}$ is a topological partition, that $\mathcal{R}_1$ is a refinement of $\mathcal{P} \vee \mathcal{Q}$, and $\mathcal{R}_2$ a partial backward refinement of $\mathcal{R}_1$. Then the under-approximation of the $\mathcal{Q}$-itineraries of f induced by $\mathcal{R}_2$ is a superset of the set of $\mathcal{Q}$-itineraries induced by $\mathcal{R}_1$.*

Proof. Suppose $I_k, J_k \in \mathcal{R}_1$ and $f(I_k) \supset J_k$. If $J_k = [c, d]$, then $a, b \in I_k$ such that $f(a, c) \subset (c, d)$ and either $f(a) = c$ and $f(b) = d$, or $f(a) = d$ and $f(b) = c$. Take a', b' such that $f(a') = c$ and $f(b') = d$ and assume $a' < b'$ (the case $a' > b'$ is similar). Let $a = \sup\{x \in [a', b'] \mid f(a) = c\}$ and $b = \inf\{x \in [a, b'] \mid f(b) = d\}$. Then clearly $f(x) \notin \{c, d\}$ for all $x \in (a, b)$. Since $\mathcal{R}_2$ is a backward refinement of $\mathcal{R}_1$, there exists an interval $I_{k+1} \in f^{-(k+1)}(\mathcal{P} \vee \mathcal{Q})$ such that $[a, b] \subset I_{k+1}$ and so $f(I_{k+1}) \supset J_k$. Hence $\exists I_{k+1} \in I_k, \forall J_{k+1} \subset J_k, f(I_{k+1}) \supset J_{k+1}$.

Now suppose $\vec{s}$ is a $\mathcal{R}_1$-itinerary, so $f(I_{k,n_i}) \supset I_{k,n_{i+1}}$ for all i for intervals $I_{k,n_i} \subset I_{s_i}$. By the above, there exist intervals I_{k+1,m_i} of $\mathcal{R}_2$ such that $I_{k+1,m_i} \subset I_{k,n_i}$ and $f(I_{k+1,m_i}) \supset I_{k,n_i}$, and immediately $f(I_{k+1,m_i}) \supset I_{k+1,m_{i+1}}$. Hence $\vec{s}$ is a $\mathcal{R}_2$-itinerary. □

We now consider the convergence of the approximation using backwards refinement. Unfortunately, it is not the case that the lower-approximation of the symbolic dynamics always converges in the Hausdorff metric.

Example 2. Let f be a function which is monotone-continuous on the partition $\mathcal{P}$ with boundary elements $p_0, \ldots, p_4$ such that $f(p_0) = p_0, p_1 < f(p_1) < f(p_2) = p_2$, and $f(p_3) = q_2, f(p_4) = q_1$ with $f(p_1) < f(q_1) < q_1 < q_2 < f(q_2) < p_2$, as shown in Fig. 1. Then $f^n([p_3, p_4]) = [f^{n-1}(q_1), f^{n-1}(q_2)] \subset (f^m(p_1), f^m(p_2))$ for all m, n, so there are no preimages of $\mathcal{P}$ in (p_3, p_4). Let J_n be the interval $(f^{-n}(p_1), p_2)$, $I_n = (f^{1-n}(p_1), f^{-n}(p_1))$ and $L = (p_4, p_5)$ Then $f(L) \subset J_n$ but $f(L) \not\supset J_n$ for all n, and $f(J_n) \supset I_n \cup J_n$. Hence there is no solid outgoing arrow from L, and L is not part of an attractor bounded by points of $f^{-n}(\partial\mathcal{P})$, so the itineraries starting in L are not captured by any lower approximation $\underline{\Sigma}(f, \mathcal{P}, \mathcal{R}_n)$.

Theorem 6. *Suppose $f : X \longrightarrow X$ is a $\mathcal{P}$-monotone-continuous map. Then the over-approximations of the $\mathcal{Q}$-symbolic dynamics computed by Algorithm 1 using backwards refinement converge to the upper symbolic dynamics of f as the precision and maximum number of steps increase.*

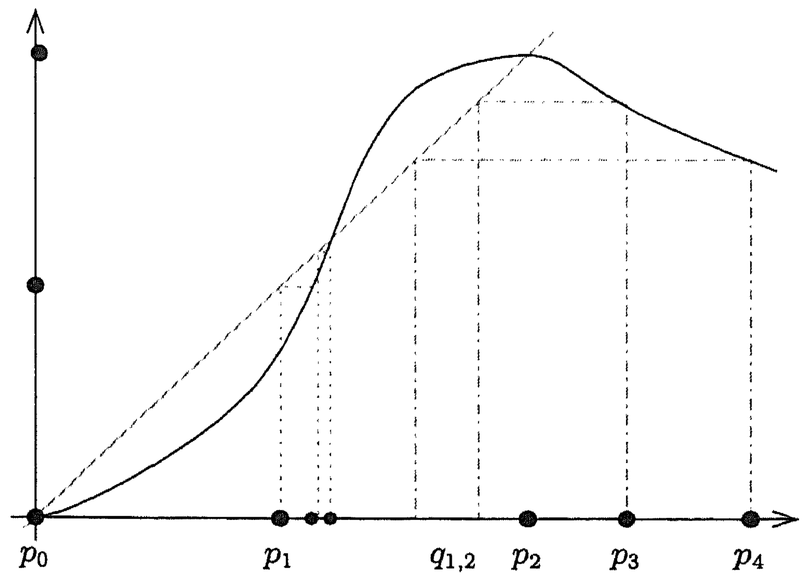

Fig. 1. A map for which the approximations of the lower symbolic dynamics computed using backwards refinement do not converge. For any stage of backward refinement, the interval $I_3 = (p_3, p_4)$ has no outgoing solid edges.

Proof. Let $\mathcal{R}_0$ be the partition into monotone-continuous branches refining $\mathcal{P} \vee \mathcal{Q}$. Let $\mathcal{R}_n$ be the refinement of $\mathcal{R}_0$ computed with n steps of the backward refinement strategy. Notice that if R is a subinterval of $\mathcal{R}_n$ whose boundary points are not in $\partial\mathcal{R}_0$, then the image of R exactly covers subintervals of $\mathcal{R}_n$.

To prove that the upper approximations converge to $\overline{\Sigma}(f, \mathcal{Q})$, suppose that $(s_0, s_1, \ldots, s_m)$ is a word which does not occur in $\overline{\Sigma}(f, \mathcal{Q})$. Then $\{x \mid f^k(x) \in Q_{s_k} \text{ for } k = 0, \ldots, m\}$ is empty. However, this set consists of unions of subintervals with endpoints in $f^{-n}(\partial\mathcal{R}_0)$. Hence by checking the itineraries of these subintervals, we can tell which points are absent.

If we do not have the ability to compute exact preimages, but $f^n(p_i^{\pm}) \neq p_j$ for all j, then for a fixed number of backward steps, by taking a high enough precision, the mapping dataset will yield a total order on the points, and we will be in the same situation as if we have exact information. There may be difficulties if $f^n(p_i^{\pm}) = p_j$ for some $p_i, p_j \in \partial\mathcal{P}$. For then the interval approximation $\lfloor x \rceil$ for some $x \in f^{-n}(p_j)$ will overlap $\lfloor p_i \rceil$. Since f is potentially discontinuous at p_i, we can not determine whether $f^{-n}(p_j)$ really has an element x near $d_i = p_i^{\pm}$. However, assuming the point x exists, we know that a neighbourhood of x intersects both intervals adjoining p_j, whereas if there were no preimage, the interval containing d_i would only intersect one interval adjoining p_j. Hence to obtain an over-approximation of the symbolic dynamics, we should assume that such a point x exists and is not equal to p_i.

Convergence of the over-approximations follows since if $x = p_i$, then all backward preimages of p_j intersect p_i. In this case, in the limit, the extra orbit is one of the pair with itinerary $\vec{k}|_{n-1}(d) \cdot \text{itin}(p_j^{\pm})$, where $\vec{k}|_{n-1}(d)$ is the word consisting of the first $n-1$ elements of the kneading sequence of d, and we itin$(p_j^{\pm})$ are the two possible itineraries of p_j. □

The proof of convergence is similar in nature to proofs of continuity of the topological entropy [8,26]. See [16, Theorem 16.3.1] for details. However, in our case, the lower and upper limits may be slightly different.

4. Computing symbolic dynamics using kneading theory

We now consider how to use the kneading theory to improve the symbolic dynamics. The basic kneading theory framework is first extended in a straightforward way to consider arbitrary regions for the symbols and maps with discontinuity points. We give some intuition on modifying kneading sequences to reduce the symbolic dynamics forced, and then present an algorithm to extend the partial kneading information obtained from the mapping dataset to full kneading information which is either forced by, or forces, the dynamics of the original map. Finally, we prove that this algorithm really does yield over- and under-approximations of the symbolic dynamics.

4.1. Kneading theory for discontinuous maps

Suppose f is $\mathcal{P}$-continuous, $\mathcal{L}$-monotone-continuous, and we wish to compute the symbolic dynamics relative to a partition $\mathcal{Q}$. For simplicity, we assume that every point $q \in \partial\mathcal{Q}$ is either known to be disjoint from $\partial\mathcal{L}$, or is known to coincide exactly with a point $l \in \partial\mathcal{L}$. We let $\mathcal{B}$ be the partition $\mathcal{L} \vee \mathcal{Q}$. We therefore consider the case that f is $\mathcal{B}$-monotone-continuous, and we are looking for symbolic dynamics relative to $\mathcal{B}$. When considering perturbations of f, we will allow perturbations which are $\mathcal{B}$-continuous, and not restricted to those which are merely $\mathcal{P}$-continuous; this means that we allow perturbations which destroy continuity at the critical points and points of $\partial\mathcal{Q}$.

Let b_i be the ith point of $\partial\mathcal{B}$ ordered along X, so that $B_i = (b_i^+, b_{i+1}^-)$. We let D be the set of boundaries of monotone-continuous branches, so $D = \{b_0^+, b_1^-, b_1^+, \ldots, b_{l-1}^+, b_l^-\}$.

We define kneading invariants $\vec{k}(d) = \text{itin}(f(d))$ for $d \in D$. If $f^n(d) \in \partial\mathcal{B}$ for some n, then $f(d)$ has two (or more) possible itineraries, and we take $\vec{k}(d) := \lim_{x \to d} \text{itin}(f(x))$ where the limit is taken through points in the same monotone-continuous branch as $d = b^{\pm}$. By the standard kneading theory, $\vec{s}$ is an itinerary of some point x under f if $\sigma^{n+1}(\vec{s})$ lies between $\vec{k}(b_{s_n}^+)$ and $\vec{k}(b_{s_n+1}^-)$ for all $n \in \mathbb{N} = \{0, 1, 2, \ldots\}$.

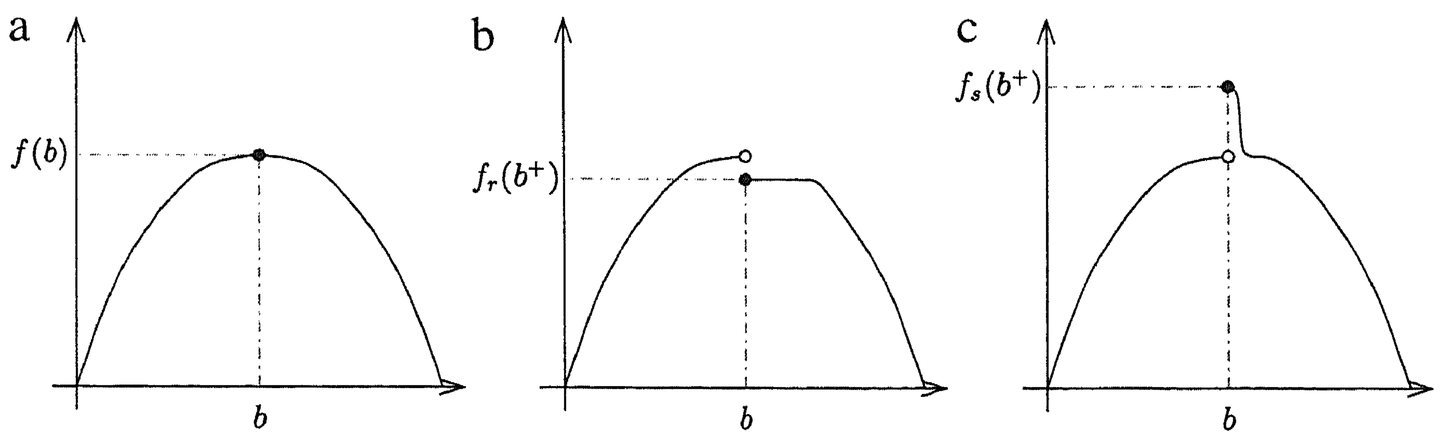

Fig. 2. Stretching and relaxing at a critical point. (a) A critical point b of f. (b) Relaxing b^+ to reduce the symbolic dynamics. (c) Stretching at b^+ to increase the symbolic dynamics.

Since we can only compute partial kneading information about points, we will be especially interested in modifications to the function f or its kneading invariants $\vec{k}_f(d)$ which either decrease or increase the symbolic dynamics. The critical observation is that if d is a maximum (the left-hand end of a decreasing branch or right-hand end of an increasing branch), then decreasing $\vec{k}(d)$ decreases the symbolic dynamics.

We let $\delta_k(d)$ for $d \in D$ be equal to $+1$ if f^k has a local minimum at d, and -1 if f^k has a local maximum at d.

4.2. Relaxing and stretching

We now give an informal analysis of homotopies and their effect on the kneading invariants.

If $d \in D$ is a discontinuity and $\vec{s}$ is an itinerary, we write $\sigma^{n-1}(\vec{k}(d)) \succ \vec{s}$ if f^n has a maximum at d and $\sigma^{n-1}(\vec{k}(d)) > \vec{s}$, or $\sigma^{n-1}(\vec{k}(d)) \succ \vec{s}$ if f^n has a minimum at d and $\sigma^{n-1}(\vec{k}(d)) < \vec{s}$. This means that relaxing f moves $f^n(d)$ towards the point x with itinerary s. If d is a discontinuity, and $\vec{k}_1$ and $\vec{k}_2$ are two possible kneading sequences for d, we write $\vec{k}_1 \prec \vec{k}_2$ if d is a maximum and $\vec{k}_1 < \vec{k}_2$, or d is a minimum and $\vec{k}_1 < \vec{k}_2$. Clearly, if f and g are two maps with the same discontinuity and critical points, and if $k_f(c_j) \prec k_g(c_j)$, then every itinerary of f is an itinerary of g.

Suppose f has a local maximum at $d = p^{\pm}$. Let f_s be a homotopy with $f_0 = f$ such that $f_s(d)$ decreases as s increases. Then images $f_s^k(d)$ move to the left if $\delta_k(d) = -1$, and to the right if $\delta_k(d) = +1$ for as long as $f_s^i(d)$ remains away from $\partial\mathcal{B}$ for $i \le k$. Intuitively, this will reduce the kneading invariant $\vec{k}_{f_s}(d)$, as long as $f_s^i(d)$ crosses $\partial\mathcal{B} \setminus b$ for some $i < j$ before $f_s^k(d)$ crosses b. For in this case, $f_s^k(d) = f^{k-1}(f_s(d)) \gtrless f^k(d)$ depending on $\delta_k(d)$.

We call a homotopy which decreases the kneading invariant $\vec{k}_{f_s}(d)$ of a maximum, or increases the kneading invariant of a minimum, a *relaxation*, and say that $\vec{k}_f(d)$ *relaxes* to $\vec{k}_{f_s}(d)$ and that d is relaxed. Similarly, a homotopy which increases the kneading invariant of a maximum, or decreases the kneading invariant of a minimum, is *stretching*.

Now suppose f^k has a maximum at $d \in D$ and that $x \in \partial\mathcal{B}$. Then we can homotope f in a neighbourhood of d to set $f_s(d) = f_s(x) = f(x)$. This will have essentially the same effect as a relaxation in a neighbourhood of d to set $f^k(f_s(d)) = f(x)$.

We define the relations $\prec$ and $\succ$ on forward images of discontinuity points by saying $f^k(d) \prec x$ if $\delta_k(d)$ has the same sign as $f^k(d) - x$, and $f^k(d) \succ x$ if $\delta_k(d)$ has the opposite sign as $f^k(d) - x$.

There is a critical difference between the locality of relaxations and stretching. For if f has a maximum at $d \in \partial B$, then to set $f_s(d) = y < f(d)$ but preserve monotonicity on B, we need to change f_s on the entire neighbourhood $[d, x]$ of d with $f(x) = y$. However, to stretch to $f_s(d) = y > f(d)$, we only need to change f_s on an arbitrarily small neighbourhood of d by introducing a very narrow "spike". Note that as shown in Fig. 2, it is not necessary to preserve continuity at b, though this could be done by relaxing or stretching at b^- as well as at b^+.

We will need the following result on forcing relations between maps due to their kneading invariants.

Theorem 7. *Let f and g be $\mathcal{B}$-monotone-continuous maps with discontinuities $D = \partial\mathcal{B}^{\pm}$. Suppose that for all discontinuities $d \in D$, either*

1. *$k_g(d) \prec k_f(d)$, where $\prec$ is $<$ when f has a maximum at d, and $>$ when f has a minimum at d.*
2. *$g^n(d) = d'$ for some d' with $\sigma^n(\vec{k}_f(d)) \succ \mathrm{itin}(d')$.*

Then every $\mathcal{B}$-itinerary of g is an itinerary of f.

Proof. Consider an itinerary $\vec{s}$ of g, and let x be a point with itinerary $\vec{s}$. Suppose $s_n = i$, so $g^n(x) \in [b_i^+, b_{i+1}^-]$. Then by the kneading condition, we have $\sigma^{n+1}(\vec{s})$ between $\vec{k}_g(b_i^+)$ and $\vec{k}_g(b_{i+1}^-)$.

If $\vec{k}_g(d)$ is determined by Condition 1 above, then $\sigma^{n+1}(\vec{s})$ has the same relation to $\vec{k}_f(d)$ as $\vec{k}_g(d)$.

If $\vec{k}_g(d)$ is determined by Condition 2, then $g^m(d) = b_j$ for some $b_j \in \partial\mathcal{B}$, and $g^l(d)$ and $f^l(d)$ lie in the same regions for $l < m$. Then if the itineraries of d and $f^n(x)$ differ in the first m symbols, then $\sigma^{n+1}(\vec{s})$ and $\vec{k}_f(d)$ differ in the first $m-1$ symbols, so the bound is satisfied. Otherwise we have $s_{m+n} \in \{j, j+1\}$, and since σ is a valid itinerary for g, so we have $\sigma^{m+n+1}(\vec{s}) \gtrless \vec{k}_g(b_j^{\pm})$. Then $\sigma^k(\vec{s})$ satisfies the kneading conditions for $k < n+m$ since the conditions are the same for f and g.

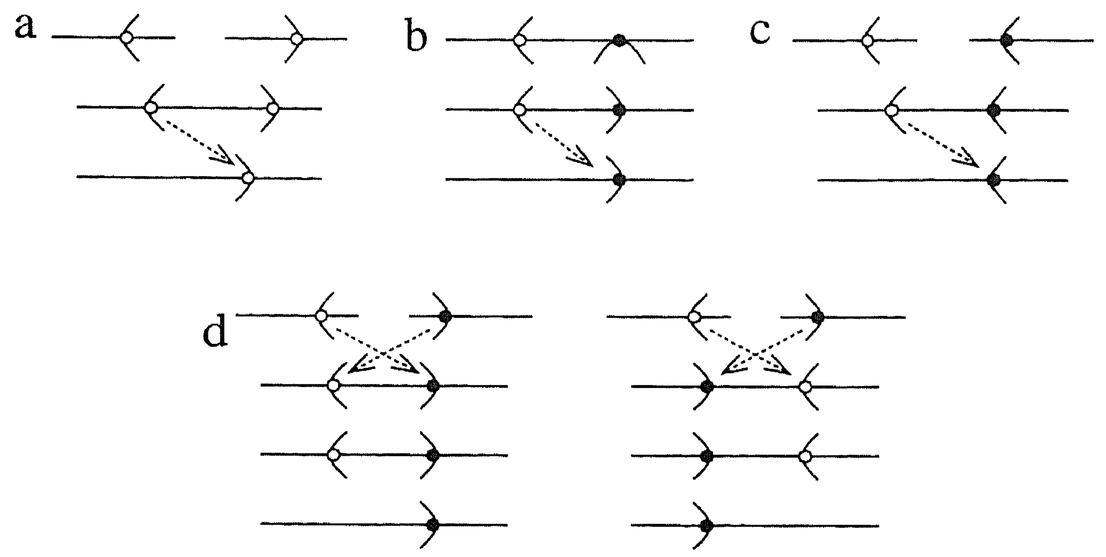

Fig. 3. Relaxations to the map g under-approximating the symbolic dynamics made in Algorithm 3.

If $\vec{k}_g(b_j^{\pm})$ is determined by Condition 1, then σ^{m+n} satisfies the kneading conditions as above. If $\vec{k}_g(b_j^{\pm})$ is also determined by Condition 2, then we need to continue until either we find a critical point determined by Condition 1, or by some iterate differing from a kneading invariant, or we have an infinite loop. □

4.3. Kneading invariants from mapping data sets

Ideally, given a mapping dataset $\mathscr{F} = (Y, f, \lfloor\cdot\rceil, \leq)$ as in Definition 6, we would like to extend the data by extending the ordering to a total ordering, and extending the mapping information to a total function, such that the resulting kneading information forces only orbits which are present in all maps consistent with the mapping data. Unfortunately, this is not always possible. We shall see examples of mapping datasets (which can be taken to be totally ordered) for which there is no extension to a total function with minimal symbolic dynamics. Instead, we need to relax the ordering on the mapping dataset in certain instances.

Given a mapping dataset, if we know the ordering of the partition boundary points Q, the discontinuity points D and the critical points C, and all their kneading sequences, then we can determine the ordering of all images of points of P. If all points of P are eventually periodic, then so are the kneading sequences, and can be determined purely from the image data.

Definition 12. Kneading invariants $\vec{k}(d)$, $d \in D$ are *consistent* with a mapping dataset $(Y, f, \lfloor\cdot\rceil, \leq)$ if

1. $\sigma^j(\vec{k}(d)) \in [\vec{k}(p^+_{k_j(d)}), \vec{k}(p^-_{k_{j'}(d)+1})]$, and
2. if $f^j(d) \geq f^{j'}(d')$, then $\sigma^j(\vec{k}(d)) \geq \sigma^{j'}(\vec{k}(d'))$.

If every kneading invariant is eventually periodic, then consistency can be checked by a finite algorithm.

In order to compute lower- and upper-approximations of the symbolic dynamics we therefore need to set the image of each $f^n(d)$ for which the image is not already given by the mapping data. By the kneading theory, we should aim to relax the kneading invariants to reduce the symbolic dynamics, and stretch kneading invariants to increase the symbolic dynamics.

If $x < y$, we say that x and y are *adjacent* if there is no point z such that $x < z$ and $z < y$.

Algorithm 3. Given a mapping dataset $\mathscr{F}$, we aim to find a map g such that any map f compatible with $\mathscr{F}$ has all the itineraries of g.

1. Choose $d \in D$ with exactly n forward images in the mapping data. Let $x = f^m(c)$ be the point adjacent to d which $f^n(d)$ relaxes to. Consider the following cases:
   (a) $d = c$. Then $f^n(d)$ and x lie in the same orbit. Extend the mapping data by setting $g(g^n(d)) = g^m(e)$.
   (b) $d \neq c$ and relaxing g at c moves $g^m(c)$ away from $g^n(d)$. Then we set $g(g^n(d)) = g^{m+1}(c)$; note that $g^{m+1}(c)$ need not be defined yet.
   (c) $d \neq c$ and $g^{n-m+i}(d)$ is adjacent to $f^i(c)$ for $i = 0, \ldots, m$. Then set $g(g^n(d)) = g^{m+1}(c)$.
   (d) $d \neq c$, $m > 0$ and relaxing g at c moves $g^m(c)$ towards $g^n(d)$. Let l be maximal such that $g^{n-i}(d)$ and $g^{m-i}(c)$ lie in the same lap for $0 \leq i \leq l$. Then remove the ordering requirement between $g^{n-i}(d)$ and $g^{m-i}(c)$.
2. Whenever $\sigma^i(\text{itin}(d)) \neq \sigma^j(\text{itin}(c))$ (i.e. the known part of the itineraries definitely differ), then add the ordering $g^i(d) \lessgtr g^j(c) g \iff \sigma^i(\text{itin}(d)) \lessgtr \sigma^j(\text{itin}(c))$.

In order to find h which forces all itineraries of f, we use the same construction, but set $h(h^n(d))$ in the direction of stretching at d, rather than relaxing (Fig. 3).

Note that if we set $g(g^n(d))$ equal to $g^{m+1}(c)$, and $g^n(d)$ and $g^m(c)$ lie in the same monotone branch, then g is constant on $[g^n(d), g^m(c)]$.

We can apply Algorithm 3 without any ordering data except for comparisons of $f^i(d)$ with c for $d, c \in D$. In this case, we obtain the dynamics forced by the symbolic itineraries. Notice that c is a critical point of f which is not a discontinuity point, then relaxing and stretching at c can be performed keeping the maps continuous.

Theorem 8. *The symbolic dynamics of the map g constructed by Algorithm* 3 *is a subshift of that of f, and the symbolic dynamics of h is a supershift of f.*

Proof. Suppose $g(f^n(d))$ is determined by (a). Then setting $g^{n+1}(d)$ to $f^{m+1}(d)$ makes d eventually periodic. Further, if f^{n-m} is orientation-reversing, then $f^{2n-m}(d)$ lies on the same side of $f^n(d)$ as does $f^m(d)$. This means that $k_g(d)$ is an itinerary of f.

Suppose $g(f^n(d))$ is determined by (b). Then $\vec{k}_g(d) \prec \vec{k}_f(d)|_{\{0,n-1\}}\sigma^{m-1}\vec{k}_g(c)$, so it satisfies Condition 2 of Theorem 7.

Suppose $g(f^n(d))$ is determined by (c). Then $\vec{k}_g(d) = \vec{k}_f(d)|_{\{0,l-1\}}\vec{k}_g(c)$. Although this may not relax $\vec{k}_f(d)$, the kneading invariant $\vec{k}_g(d)$ satisfies Condition 2 of Theorem 7.

Suppose we are in the situation of (d). Then the kneading invariant $\vec{k}_g(d)$ is not determined, but since we remove some ordering relations, the symbolic dynamics must decrease for g. □

We now give an example of a map f with a mapping dataset computed using forward refinement which does not admit a representative with minimal symbolic dynamics.

Example 3. Let $X = [0, 3]$, and $\mathcal{Q}$ be the partition with endpoints $\left\{0, \frac{1}{3}, \frac{2}{3}, 1, 2, 2\frac{1}{3}, 2\frac{2}{3}, 3\right\}$. Let f be a system such that $f(0) = 1, f(1) = 2, 1 = f(0) < f\left(\frac{2}{3}\right) < f\left(\frac{1}{3}\right) < f(1) = 2$, and $f(2) = f\left(2\frac{2}{3}\right) = 3, f\left(2\frac{1}{3}\right) = f(3) = 2$. Define symbols $q_i = \left[\frac{i}{3}, \frac{i+1}{3}\right]$ and $q_{i+4} = \left[2\frac{i}{3}, 2\frac{i+1}{3}\right]$ for $i = 0, 1, 2$, and $q_3 = [1, 2]$.

Then since $f(I_0) \cup f(I_2) = I_3$ and $f(I_3) = f(I_4) = f(I_5) = f(I_6) = I_4 \cup I_5 \cup I_6$, we know that for any sequence $\vec{s} \in \{4, 5, 6\}^\omega$, there exists a point with itinerary $03\vec{s}$ or $23\vec{s}$. However, by taking $f\left(\frac{1}{3}\right)$ very close to $f(0)$, we can rule out the itinerary $03\vec{5}$, whereas taking $f\left(\frac{2}{3}\right)$ very close to $f(1)$, we can rule out the itinerary $23\vec{s}$ (as long as $\vec{s}$ is not either $\overline{4}$ or $\overline{6}$).

4.4. The kneading algorithm for unimodal maps

Let f be a unimodal map on $[a, b]$ with $f(b) = f(a) = a$ and single critical point at c. Let $P_0 = (a, c)$ and $P_1 = (c, b)$. The computation of the topological entropy using kneading data for unimodal maps has been considered in [27,28]. When applying Algorithm 3 we are always in case (a) of choosing the image of $f^n(c)$. This means that if $f^i(c) < f^n(c) < f^j(c)$ and f^n have a maximum at c, then we set $g(f^n(c)) = f^{i+1}(c)$, and $h(f^n(c)) = f^{j+1}(c)$. In the former case, we collapse the interval $[f^i(c), f^n(c)]$ and map $[f^n(c), f^j(c)]$ to $[f^{i+1}(c), f^{j+1}(c)]$. The resulting kneading sequence is eventually periodic, and may be periodic if $f^n(c)$ relaxes onto c itself. If the mapping data does not give a total order on the images of c, then we may be able to deduce some of the ordering from the kneading invariant.

The following example shows that just relying on the kneading sequences can lose information.

Example 4. Consider a unimodal map f with $c_2 < c_3 < c_5 < c_0 < c_4 < c_1$, where $c_i = f^i(c)$. Then $c_4 < c_6 < c_1$, $c_2 < c_7 < c_5$ and $c_3 < c_8 < c_1$, so the kneading sequence is $1001010?? \cdots$.

Continuing the kneading sequence in a consistent way with as little dynamics as possible gives $\vec{k} = \overline{1001010}$, which induces topological entropy 0.522. However, for this kneading invariant, the itinerary of c_3 is $010101 \cdots$ and the itinerary of c_5 is $010100 \cdots$ which is lower. Hence the kneading information is not consistent with the interval information.

If we are to respect the condition $c_3 < c_5$, then we can only change the kneading sequence to $100\overline{1}$, in which c_3 and c_5 have the same periodic itinerary, and which induces topological entropy 0.528.

5. Examples

We now give some simple examples illustrating the main features of the paper and the results of our algorithms. We consider the quadratic unimodal map

$$f(x) = \mu x(1 - x),$$

the cubic bimodal map

$$f(x) = ax + (1 - a - b)x^2 + bx^3$$

and the normal form of a discontinuous border-collision bifurcation of a stable fixed-point with a square-root singularity [29].

$$f(x) = \begin{cases} ax + \epsilon & \text{if } x \leq 0; \\ \sqrt{bx - c} & \text{if } x \geq 0. \end{cases} \tag{1}$$

5.1. The unimodal map

Consider the unimodal map:

$$f(x) = \mu x(1 - x) \quad \text{with } \mu = 3.92.$$

Let $a = 0$ and $b = 1$ be the endpoints of the interval I and $c = 0.5$ be the critical point. Let $I_0 = [a, c]$ and $I_1 = [c, b]$.

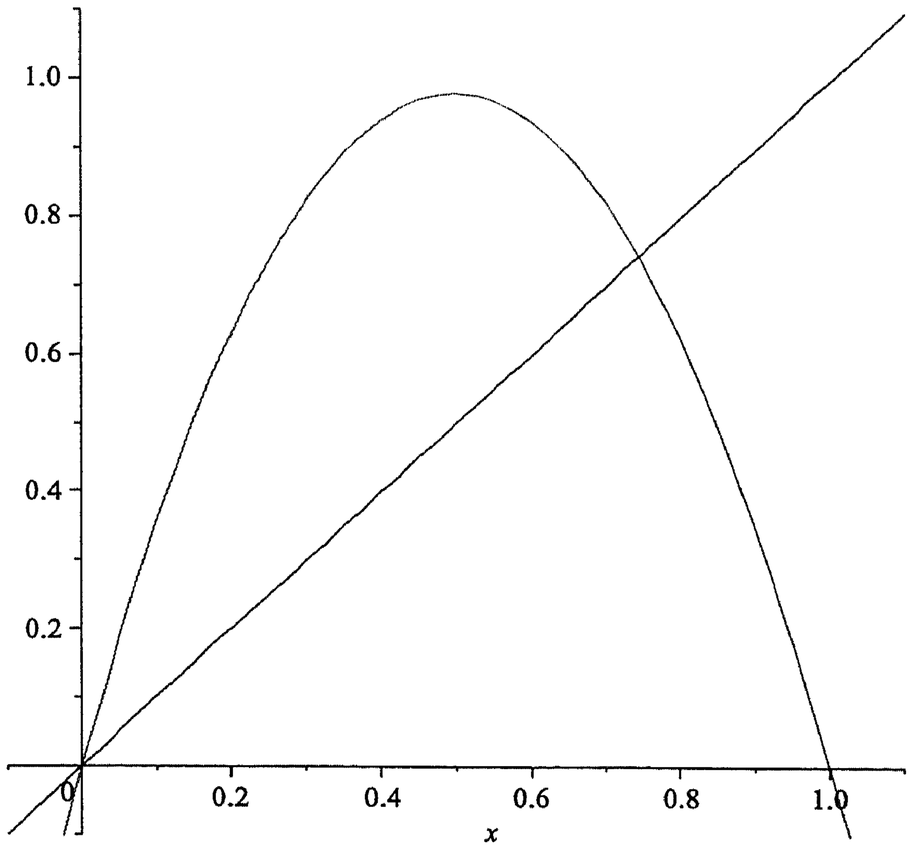

Fig. 4. Unimodal map.

The orbit of the critical point is given by $f^i(c) = c_i$ with

$$c_0 = 0.5, \quad c_1 = 0.98, \quad c_2 \approx 0.077, \quad c_3 \approx 0.278, \quad c_4 \approx 0.787,$$
$$c_5 \approx 0.657, \quad c_6 \approx 0.883, \quad c_7 \approx 0.405, \quad c_8 \approx 0.945, \quad c_9 \approx 0.204.$$

The itinerary of $f(c)$ is therefore

$$\text{itin}(f(c)) = 100111010\cdots.$$

Consider the partition into six intervals with boundary points

$$p_0 = a, \quad p_1 = c_2, \quad p_3 = c_3, \quad p_4 = c_0, \quad p_5 = c_4, \quad p_6 = c_1, \quad p_7 = b.$$

Note that $f(p_5) \in (p_4, p_5)$. Taking $J_i = [p_i, p_{i+1}]$ we have

$$f(J_1) \supset J_2 \cup J_3; \quad f(J_2) \supset J_4; \quad f(J_3) \supset J_4; \quad f(J_4) \supset J_1 \cup J_2$$

and also

$$f(J_3) \cap J_3 \neq \emptyset \quad \text{and} \quad f(J_4) \cap J_3 \neq \emptyset.$$

Now consider the computation of entropy. Using the lower and upper symbolic dynamics on the partition, we obtain entropies of 0.41962 and 0.73286. The upper shift on the refined partition has multiple orbits with the same itinerary on I_0 and I_1. If we consider the entropy of the shift itself (by using additional states J_{12} and J_{34}) we obtain 0.583.

Improvement of entropy using kneading theory

If we use the kneading theory, we see that by setting $f(c_4) = c_4$ we have $\text{itin}(f(c)) = 1001111\cdots$ which is higher in the unimodel order, and setting $f(c_4) = c_0$ we have $\text{itin}(f(c)) = 1001^0_1100\cdots$ which is lower than $10011101\cdots$. The corresponding lower and upper entropies are 0.54354 and 0.571.

Consider a unimodal map with kneading invariant $\overline{1001^0_1}$, so c is periodic and $f^5(c) = c$. The images of c are ordered $a < f^2(c) < f^3(c) < c < f^4(c) < f(c) < b$. We can compute the topological entropy of the shift and obtain a value of 0.54354.

Consider a unimodal map with kneading invariant $100\bar{1}$, so c is eventually periodic and $f^5(c) = f^4(c)$. The images of c are ordered $a < f^2(c) < f^3(c) < c < f^4(c) < f(c) < b$. We can compute the topological entropy of the shift, and obtain a value of 0.57058.

Now consider a unimodal map with kneading invariant $\vec{k} = 10011\cdots$. From the kneading theory, we know $10011 \succ 1001^0_1$ so we have $h_{\text{top}}(f) \geq 0.64$. Define $R_1 = [f^2(c), f^3(c)]$, $R_1 = [f^3(c), c]$, $R_3 = [c, f^4(c)]$ and $R_4 = [f^4(c), f(c)]$. When using the forward refinement strategy, since $f^5(c) \in R_3$, the interval R_3 maps to $[f^5(c), f(c)]$ and the interval $[f^4(c), f(c)]$ maps to $[f^2(c), f^5(c)]$ which together cover R_3, but neither does individually. Hence neither of the transitions $R_3 \longrightarrow R_3$ nor $R_4 \longrightarrow R_3$ in the automaton for the lower symbolic dynamics. The entropy bound obtained drops to 0.41962.

The overall effect of the kneading theory is to "choose" a transition, either $R_3 \longrightarrow R_3$ or $R_4 \longrightarrow R_3$, to put in the lower symbolic dynamics, while still ensuring that the dynamics are a lower bound. The chosen transition is the one giving the least entropy (Fig. 4).

Table 1
Entropy of the unimodal map using backward and hybrid refinement.

Steps	Entropy	Running time backward	Running time hybrid
1	[0:0.69314]	0.05	0.11
2	[0.48121:0.69315]	0.11	0.12
3	[0.48121:0.60938]	0.24	0.26
4	[0.54353:0.60938]	0.55	0.58
5	[0.54353:0.58356]	1.26	1.21
6	[0.54353:0.56240]	2.68	2.63
7	[0.54761:0.56240]	6.73	5.74
8	[0.55642:0.56240]	17.74	11.04
9	[0.55642:0.56099]	49.32	18.86
10	[0.55842:0.56099]	149.26	30.44
11	[0.55990:0.56099]	450.37	47.78
12	[0.55990:0.56073]	1246.19	76.07
13	[0.55990:0.56026]		116.80
14	[0.55998:0.56026]		186.57
15	[0.56014:0.56026]		309.09

Table 2
Entropy of the unimodal map with kneading algorithm.

Steps	Entropy	Running time
1	[0:0.693147180559]	0.01
2	[0:0.693147180559]	0.04
3	[0.481211825059:0.6931471805599]	0.03
4	[0.481211825059:0.6093778634360]	0.03
5	[0.543535072497:0.5705796667792]	0.06
6	[0.543535072497:0.5705796667792]	0.10
7	[0.555194599694:0.5623991486459]	0.10
8	[0.557934930430:0.5623991486459]	0.10
9	[0.558939519816:0.5623991486459]	0.13
10	[0.560046256097:0.560988810813]	0.10
15	[0.560216078753:0.560259207813]	0.09
20	[0.560235149472:0.560235821005]	0.16
25	[0.560235528970:0.560235669923]	0.20
30	[0.560235632260:0.560235638765]	0.27
35	[0.560235635949:0.560235636493]	0.36
40	[0.560235636370:0.560235636375]	0.55

5.2. A bimodal map

$$f(x) = 0.35x^3 - 2.75x^2 + 4.5x + 3.3.$$

The initial partition has the following end-points: $\text{fix}_0 \approx -0.619$, $c_0 \approx 1.015$, $c_1 \approx 4.223$, $fix_2 \approx 5.886$.

5.3. A discontinuous border-collision

A discontinuous border-collision bifurcation of a stable fixed-point with a square-root singularity gives the following normal form [29].

$$f(x) = \begin{cases} ax + \epsilon & \text{if } x \leq 0; \\ \sqrt{bx} - c & \text{if } x \geq 0. \end{cases} \tag{2}$$

$a = -3.5, e = 1.5, b = 2, c = 2.$

5.4. Comparison of different strategies

In this section we compare the effectiveness of different refinement strategies and methods for extracting the symbolic dynamics.

In Table 1 after the seventh steps the running time increases by a factor which ranges over the interval [2.5, 3] for backward refinement while with a factor which ranges over the interval [1.5, 1.7] for hybrid refinement (Table 2). In Table 3 after the fifth steps the running time increases by a factor which ranges over the interval [4.5, 4.6] for backward refinement while with a factor which ranges over the interval [1.7, 2] for hybrid refinement.

These observations suggest that the running time follows an exponential law in terms of the steps of refinement, in the hybrid refinement the exponential rate is lower than with the backward refinement. This outcome matches the structure

Table 3
Entropy of the bimodal map with backward and hybrid refinement.

Steps	Entropy	Running time backward	Running time hybrid
1	[0:0.88137]	0.20	0.26
2	[0.69314:0.83412]	0.77	0.82
3	[0.75832:0.81443]	1.15	1.23
4	[0.77727:0.80327]	3.66	3.52
5	[0.77727:0.78803]	12.65	8.80
6	[0.78109:0.78636]	51.15	19.97
7	[0.78303:0.78533]	233.61	42.91
8	[0.78351:0.78463]	1057.99	83.19
9	[0.78383:0.78441]		141.64
10	[0.78408:0.78425]		279.64

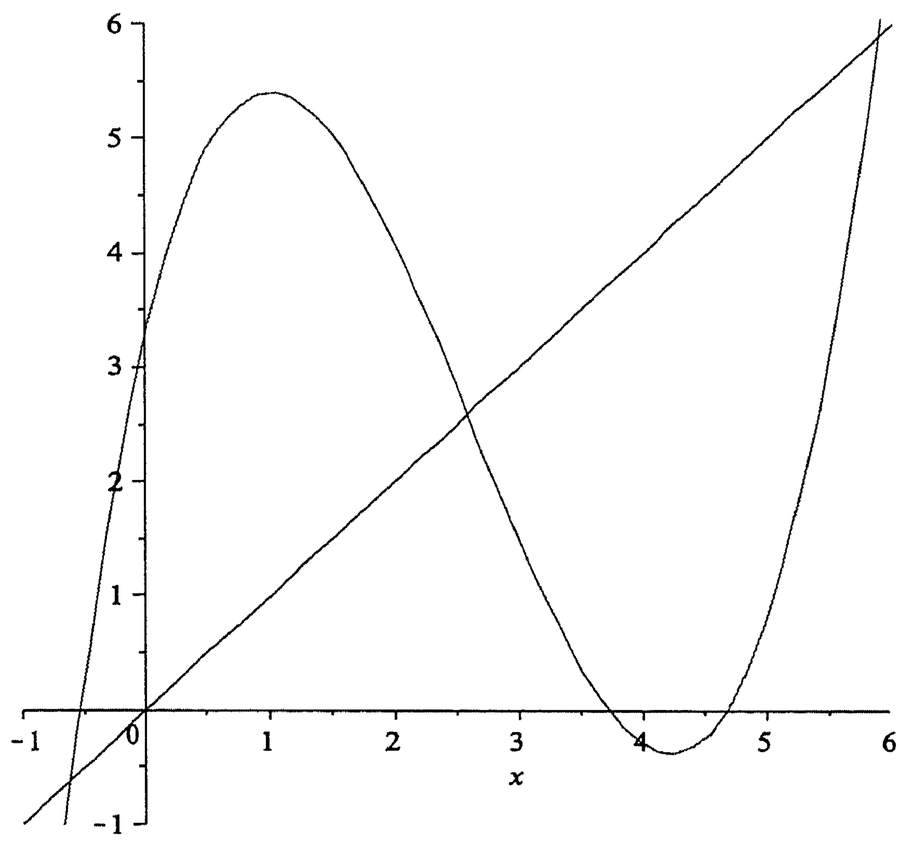

Fig. 5. Bimodal map.

of the algorithms where in both cases we need to deal with exponentially growing number of preimages of endpoints as we said in Section 3.2. The hybrid approach is faster because filter out most of the endpoints obtaining a partition whose cardinality grows linearly.

Instead, in the forward refinement kneading approach the data approximatively match a liner function for the running time in terms of the steps. This algorithm is much faster because on the one hand the computation of forward images is easier then backward images, and on the other hand the number of endpoints increases linearly.

In all these three approaches the accuracy of the entropy approximation increases monotonically, despite not always being strictly monotonically. Finding an exact law which expresses the rate of convergence of the computation of topological entropy in terms of the steps of refinement and the running time is not straightforward. This problem requires further investigation and the authors' guess is that it deeply depends on the structure of the map.

6. Case studies

In this section, we present three case studies: a discontinuous border-collision singularity, a simple hysteresis system and the singular limit of the Van der Pol equation (Fig. 5).

6.1. A hysteresis switching system

We now consider a piecewise-affine model of a system governed by hysteresis switching [30]. Let $H(x)$ be the hysteresis map, informally given by $H(x) = 0$ for $x \leq 1$ and $H(x) = 1$ for $x \geq 0$. Consider the system:

$$\begin{aligned} \dot{x} &= y + a_1 H(x/b) \\ \dot{y} &= -x - 2\sigma y + a_2 H(x/b). \end{aligned} \tag{3}$$

The return map is defined on the set $P = \{(x, y) \in \mathbb{R}^2 \mid x = 0,\ y > 0\}$ as: $f(p) = \phi(p, \bar{t})$ where $\bar{t} = \min_t\{t \mid q = \phi(p, t) \in P \text{ and } H(x_q) = 0\}$ and $\phi(p, t)$ is the integral map of the system (3). We have computed symbolic dynamics for the

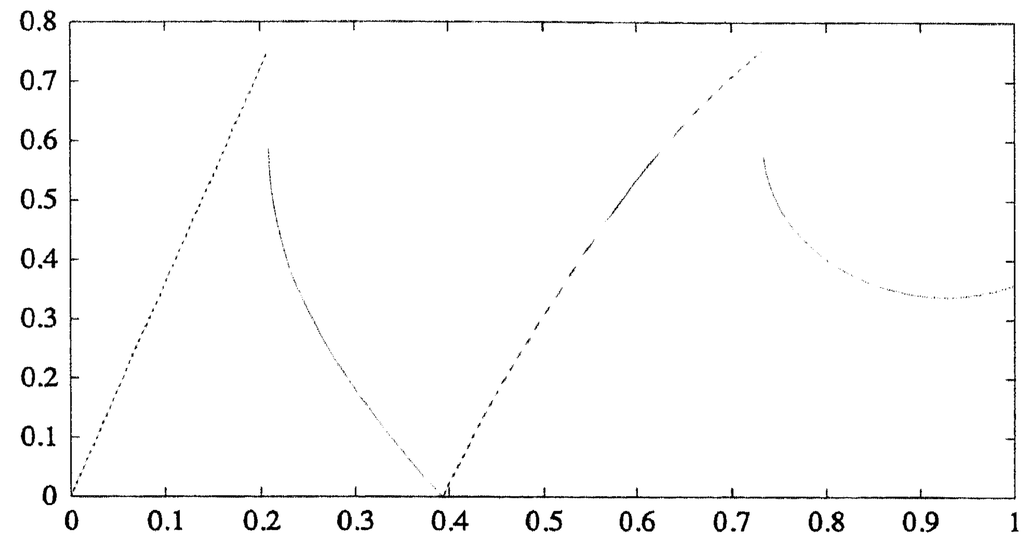

Fig. 6. The return map for the hysteresis system (3).

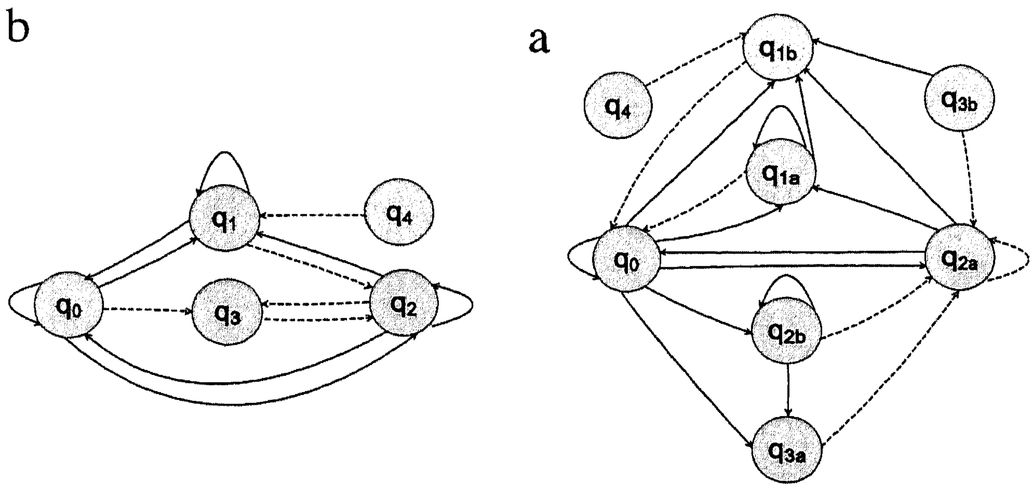

Fig. 7. Lower and upper approximation of symbolic dynamics for the hysteresis system (3) for (a) the initial partition and (b) the forward refinement of the initial partition.

return map with parameter values $a_1 = -1, a_2 = -1, b = 0.3$ and $\sigma = -0.2$. The graph of the return map is shown in Fig. 6. We take an initial partition $\mathcal{Q}$, which are the domains of the monotone branches. The partition elements are $Q_0 = [p_0, p_1]$, $Q_1 = [p_1, p_3]$, $Q_2 = [p_3, p_5]$, $Q_3 = [p_5, p_7]$ and $Q_4 = [p_7, p_8]$ where the boundary points are

$$p_0 = 0.0, \qquad p_1 \approx 0.20894, \qquad p_3 \approx 0.39278, \qquad p_5 \approx 0.73329, \qquad p_7 \approx 0.92580, \qquad p_8 = 1.0.$$

The associated symbolic dynamics are in Fig. 7(a). The two points of discontinuity are p_1 and p_5 and they can be proved to have the same left and right images. The partition after one iteration of forward refinements has the following additional endpoints:

$$p_2 = f(p_7) \approx 0.33792, \qquad p_4 = f(p_1^+) = f(p_5^+) \approx 0.59890, \qquad p_6 = f(p_1^-) = f(p_5^-) \approx 0.75340.$$

The symbolic dynamics generated by this partition are approximated by the graph in Fig. 7(b).

We notice that the lower approximation of the dynamics of the refined partition misses some sequences of the lower approximation of dynamics of the initial partition. This is due to the fact that although region $Q_1 = [p_1, p_3]$ covers $Q_0 = [p_0, p_1]$ under one iterate of the return map, neither of the subdivided regions $P_{1;0} = [p_1, p_2]$ and $P_{1;1} = [p_2, p_3]$ cover Q_0. Hence the convergence of the lower approximations of the symbolic dynamics computed using forward refinement is not monotone. With backward refinement the convergence can be shown to be monotone, but backward refinements have the disadvantage of being slower to compute than forward refinements (Tables 4 and 5).

The lower shift for the initial partition can be written as the regular expression

$$(q_0^* q_2)^*(q_0^\omega + q_1^\omega) + (q_0^* q_2 q_0)^*(q_1^\omega + q_2^\omega) + (q_0^* q_2)^\omega.$$

We can see for instance that the periodic sequence $(q_0 q_3 q_2 q_1)^\omega$ belongs to the upper shift but not to the lower shift. From the two shifts we can show that the topological entropy lies in the interval [0.80958, 1.27020].

The topological entropies obtained for further refinement are shown in Table 6. In Table 7 we show instead the much more accurate results obtained using the kneading approach.

6.2. The Van der Pol equation

The forced Van der Pol equation is a non-linear ordinary differential equation modeling oscillation in a vacuum tube triode circuit. Bifurcations in the singular limit of the forced Van der Pol oscillator have been studied in [31]. In this paper we analyse the following version of the equation:

$$\ddot{x} + \mu(x^2 - 1)\dot{x} + x = a(x^2 - 1)\sin(2\pi\nu\tau) \tag{4}$$

Table 4
Entropy of the bimodal map with kneading algorithm.

Steps	Entropy	Running time
1	[0:1.098612288668]	0.01
2	[0:0.881373587019]	0.01
3	[0.6931471806139:0.7949452427288]	0.05
4	[0.7641997080283:0.7949452427288]	0.06
5	[0.7772705789959:0.7949452427288]	0.06
6	[0.7772705789959:0.7880304603014]	0.07
7	[0.7825090975765:0.7847829456947]	0.10
8	[0.7839408308854:0.7844986535653]	0.12
9	[0.7840431481027:0.7844184271750]	0.14
10	[0.7840949704856:0.7842660362345]	0.16
15	[0.7841523953806:0.7841538593989]	0.31
20	[0.7841531278765:0.7841531492005]	0.51
25	[0.7841531371710:0.7841531375475]	0.71
30	[0.7841531373109:0.7841531373218]	1.02
35	[0.7841531373175:0.7841531373177]	1.50

Table 5
Entropy of the discontinuous border-collision map with kneading algorithm.

Steps	Entropy	Running time
1	[0:0.481211]	0.02
2	[0:0.481211]	0.02
3	[0, 0.240606]	0.09
4	[0, 0.240606]	0.10
5	[0, 0.240606]	0.10
6	[0, 0.240606]	0.12
7	[0, 0.240606]	0.17
8	[0, 0.240606]	0.26
9	[0, 0.227270]	0.28
10	[0, 0.227270]	0.17
15	[0.214105, 0.221197]	0.23
20	[0.217382, 0.218459]	0.41
25	[0.217429, 0.217601]	0.75
30	[0.217535, 0.217601]	0.87
35	[0.217540, 0.217561]	1.21
40	[0.217547, 0.217559]	1.89

Table 6
Entropy of the return map of the hysteresis system with forward refinement.

Steps	Entropy
3	[0.97494, 1.26249]
5	[1.02407, 1.18582]
7	[1.04636, 1.16493]
12	[1.06873, 1.15087]

Table 7
Entropy of the return map of the hysteresis system with kneading algorithm.

Steps	Entropy with kneading algorithm
1	[1.05757681, 1.14673525]
2	[1.09861228, 1.11532470]
3	[1.10409066, 1.10921416]
4	[1.10732895, 1.10921416]
5	[1.10763700, 1.10800210]
6	[1.10770695, 1.10783470]
7	[1.10777981, 1.10780229]
8	[1.10779612, 1.10780078]
9	[1.10779674, 1.10780027]
10	[1.10779826, 1.10779894]

in the singular limit as $\mu \to \infty$. To obtain a form more convenient for analysis, we rescale time $t = \tau/\mu$, introduce new parameters $\varepsilon = \frac{1}{\mu^2}$, $\omega = \nu\mu$ and $\theta = \omega t$, and define the new variable $y = \dot{x}/\mu^2 + x^3/3 - x$. We obtain the following autonomous system:

$$\varepsilon\dot{x} = y + x - x^3/3; \tag{5}$$

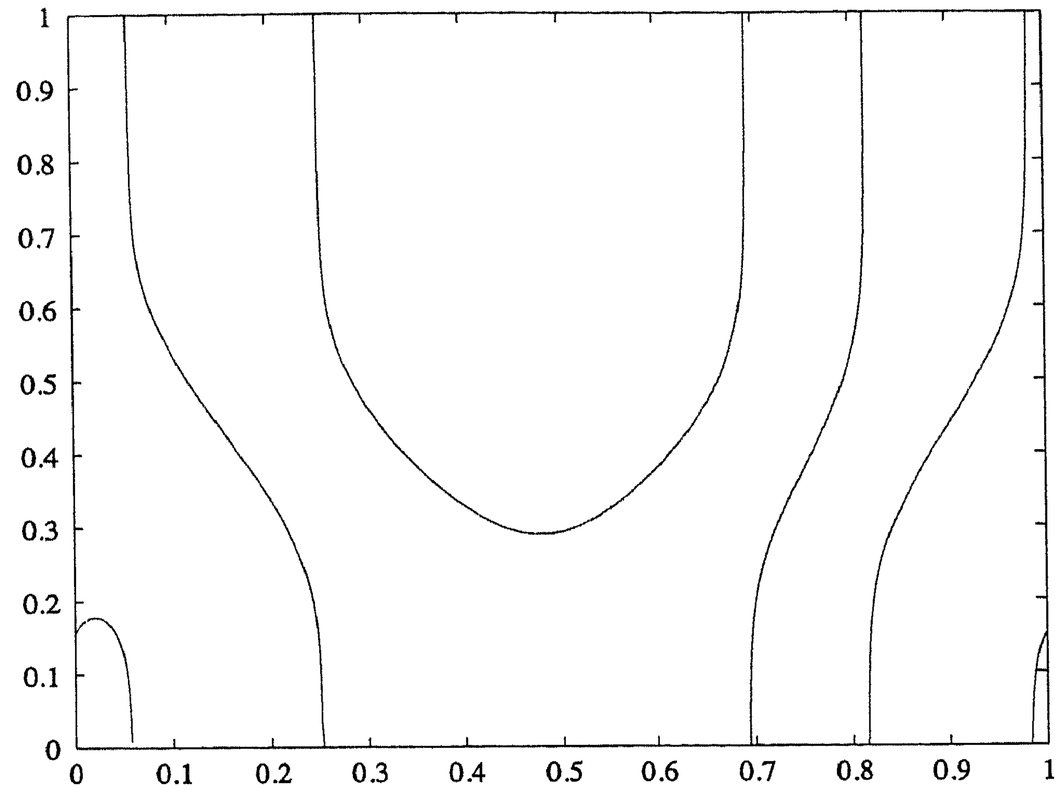

Fig. 8. The half return map for the singular limit of the forced Van der Pol oscillator (7).

$$\begin{aligned} \dot{y} &= -x + a(x^2 - 1)\sin(2\pi\theta); \\ \dot{\theta} &= \omega. \end{aligned} \tag{6}$$

The *fast subsystem* is defined by (5), since the dynamics of the fast variable x occur on a time scale which is fast relative to the evolution of the *slow variables* y and θ.

We see that on the *critical manifold* $y + x - x^3/3 = 0$ the system evolves on a time scale of order t. However, the critical manifold is unstable for the fast system if $|x| \leq 1$, and that when this occurs, the value of x jumps instantaneously to one of the stable fixed points of (5).

We can therefore view the singular limit as a hybrid system in which the continuous dynamics are given by the slow flow on the stable sheet of the critical manifold, and the reset map is given by the fast flow. By eliminating y, we obtain the following dynamics for the slow subsystem:

$$\begin{aligned} \dot{x} &= -x + a(x^2 - 1)\sin(2\pi\theta) \\ \dot{\theta} &= \omega(x^2 - 1). \end{aligned} \tag{7}$$

The fast dynamics are described by the guard set and reset map

$$G = \{(x, \theta) \mid |x| = 1\}; \qquad r(x, \theta) = (-2\,\mathrm{sgn}(x), \theta). \tag{8}$$

In other words, when the guard condition $|x| = 1$ becomes satisfied the state jumps to $x = \mp 2$.

Since the dynamics are symmetric under the transformation $T(x, \theta) = (-x, \theta + 1/2)$, we can post-compose the return map from the guard set $x = 1$ to the guard set $x = -1$ with T to obtain the *half return map* f taking $\{(r, \theta) \mid r = 1\}$ into itself. The graph of the half return map for parameter values $a = 5$ and $\omega = 3$ is shown in Fig. 8. We have computed the lower and upper symbolic dynamics with respect to the partition given by the continuous branches using forward refinement.

In the return map there are 5 discontinuity points:

$$p_2 \approx 0.05816, \qquad p_3 \approx 0.25226, \qquad p_5 \approx 0.69356, \qquad p_6 \approx 0.81553, \qquad p_7 \approx 0,98495,$$

and 2 critical points, a local maximum $p_1 \approx 0.02183$ and a local minimum $p_4 \approx 0.47872$. These points with the extremes of the interval $p_0 = 0$ and $p_8 = 1$ generate an initial partition of 9 pieces. After one forward iteration we obtain 11 pieces.

$$q_0 = f(p_0) \approx 0.15520, \qquad q_1 = f(p_1) \approx 0.17825, \qquad q_2 = f(p_4) \approx 0.29017.$$

The lower and upper discrete automata are not included for reasons of space. After one step of refinement, the discrete automaton representing the symbolic dynamics separate into two strongly connected components. Both the lower and upper shifts include the component with the highest entropy, while the lower shift does not include the smallest.

Therefore the topological entropies of the lower and upper shifts are equal and can be computed exactly yielding a numerical value of approximately 1.55705. From Fig. 8 we could already infer the entropy is at least $\log(3) \approx 1.09861$, because there are 3 continuous pieces of the partition which map the whole interval. From numerical computation we can deduce the existence of an attracting periodic orbit close to the local minimum. This lets us infer the existence of a chaotic invariant Cantor set, every point non belonging to this set converges to the attracting periodic orbit.

7. Conclusions and further research

In this paper we have considered the computation of symbolic dynamics relative to an arbitrary partition for piecewise-monotone-continuous maps of the interval. We have considered the case in which images and preimages cannot be computed exactly, but only approximations using interval arithmetic. We have considered both forwards and backwards refinements of the initial partition into monotone branches, and the computation of symbolic dynamics using both covering relations and kneading theory. We have given a number of illustrative examples from the unimodal and trimodal families, and two case studies.

As mentioned in the introduction, an important motivation for this work was to gain intuition in methods for computing symbolic dynamics in a simple case, in the hope that some of this can be carried over to higher dimensions. The backward refinement strategy for computing the upper symbolic dynamics can be carried directly over to higher dimensions. As we have seen, the entropy bounds for the sofic shift are typically very good, but care must be taken to reduce the dynamics of the generating directed graph.

Computing the lower symbolic dynamics with a convergence in entropy is complicated in higher dimensions since we can prove the existence of orbits without the covering relation. Further, the work of Misiurewicz [32] shows that the topological entropy is not lower-semicontinuous for non-invertible maps in two dimensions, and invertible maps in three dimensions. This suggests that the computable lower symbolic dynamics even in the non-invertible two-dimensional case may not match the actual dynamics present.

References

[1] O.M. Šarkovs'kiĭ, Co-existence of cycles of a continuous mapping of the line into itself, Ukrain. Math. Zh. 16 (1964) 61–71.
[2] J. Milnor, W. Thurston, On iterated maps of the interval, in: Dynamical Systems, College Park, MD, 1986–87, in: Lecture Notes in Math., vol. 1342, Springer, Berlin, 1988, pp. 465–563.
[3] L. Block, J. Keesling, Computing the topological entropy of maps of the interval with three monotone pieces, J. Stat. Phys. 66 (3–4) (1992) 755–774.
[4] J.P. Lampreia, J. Sousa Ramos, Trimodal maps, Internat. J. Bifur. Chaos Appl. Sci. Engrg. 3 (6) (1993) 1607–1617.
[5] J.L. Rocha, J. Sousa Ramos, On iterated maps of the interval with holes, J. Difference Equ. Appl. 9 (3–4) (2003) 319–335. Dedicated to Professor Alexander N. Sharkovsky on the occasion of his 65th birthday.
[6] J.F. Alves, J. Sousa Ramos, Kneading theory for tree maps, Ergodic Theory Dynam. Systems 24 (4) (2004) 957–985.
[7] J. Milnor, Is entropy effectively computable, www.math.sunysb.edu/jack/comp-ent.ps.
[8] M. Misiurewicz, Horseshoes for mappings of the interval, Bull. Acad. Pol. Sci., Ser. Sci. Math. 27 (2) (1979) 167–169.
[9] L. Block, An example where topological entropy is continuous, Trans. Amer. Math. Soc. 231 (1) (1977) 201–213.
[10] M. Misiurewicz, W. Szlenk, Entropy of piecewise monotone mappings, Studia Math. 67 (1) (1980) 45–63.
[11] R.E. Moore, Interval Analysis, Prentice-Hall Inc., Englewood Cliffs, NJ, 1966.
[12] L. Jaulin, M. Kieffer, O. Didrit, É. Walter, Applied Interval Analysis, Springer-Verlag, London, 2001.
[13] O. Aberth, Introduction to Precise Numerical Methods, Academic Press, 2007.
[14] D. Lind, B. Marcus, An Introduction to Symbolic Dynamics and Coding, Cambridge University Press, Cambridge, 1995.
[15] B.P. Kitchens, Symbolic Dynamics: One-sided, Two-sided and Countable State Markov Shifts, in: Universitext, Springer-Verlag, Berlin, 1998.
[16] A. Katok, B. Hasselblatt, Introduction to the modern theory of dynamical systems, in: Encyclopedia of Mathematics and its Applications, vol. 54, Cambridge University Press, Cambridge, 1995.
[17] V. Baladi, D. Ruelle, An extension of the theorem of Milnor and Thurston on the zeta functions of interval maps, Ergodic Theory Dynam. Systems 14 (4) (1994) 621–632.
[18] C. Preston, What you need to know to knead, Adv. Math. 78 (2) (1989) 192–252.
[19] M. Misiurewicz, K. Ziemian, Horseshoes and entropy for piecewise continuous piecewise monotone maps, in: From Phase Transitions to Chaos, World Sci. Publ., River Edge, NJ, 1992, pp. 489–500.
[20] M. Mori, Fredholm determinant for piecewise linear transformations, Osaka J. Math. 27 (1) (1990) 81–116.
[21] J.F. Alves, J. Sousa Ramos, Kneading theory: A functorial approach, Comm. Math. Phys. 204 (1) (1999) 89–114.
[22] J.P. Lampreia, J. Sousa Ramos, Symbolic dynamics of bimodal maps, Port. Math. 54 (1) (1997) 1–18.
[23] J.L. Rocha, J.S. Ramos, Weighted kneading theory of one-dimensional maps with a hole, Int. J. Math. Math. Sci. (37–40) (2004) 2019–2038.
[24] Z.X. Chen, Z. Zhou, Entropy invariants. I. The universal order relation of order-preserving star products, Chaos Solitons Fractals 15 (4) (2003) 713–727.
[25] Z.X. Chen, Z. Zhou, Entropy invariants. II. The block structure of Stefan matrices, Chaos Solitons Fractals 15 (4) (2003) 729–742.
[26] Y. Yomdin, Volume growth and entropy, Israel J. Math. 57 (3) (1987) 285–300.
[27] P. Collet, J.P. Crutchfield, J.P. Eckmann, Computing the topological entropy of maps, Comm. Math. Phys. 88 (2) (1983) 257–262.
[28] L. Block, J. Keesling, S.H. Li, K. Peterson, An improved algorithm for computing topological entropy, J. Statist. Phys. 55 (5–6) (1989) 929–939.
[29] H.E. Nusse, J.A. Yorke, Border-collision bifurcations for piecewise smooth one-dimensional maps, Internat. J. Bifur. Chaos Appl. Sci. Engrg. 5 (1) (1995) 189–207.
[30] R.W. Newcomb, N. El-Leithy, Chaos generation using binary hysteresis, Circuits Systems Signal Process. 5 (3) (1986) 321–341.
[31] J. Guckenheimer, K. Hoffman, W. Weckesser, The forced van der Pol equation. I. The slow flow and its bifurcations, SIAM J. Appl. Dyn. Syst. 2 (1) (2003) 1–35 (electronic).
[32] M. Misiurewicz, On non-continuity of topological entropy, Bull. Acad. Pol. Sci., Ser. Sci. Math. Astron. Phys. 19 (1971) 319–320.